

THESIS

SPATIAL AND TEMPORAL VARIABILITY IN CHANNEL SURFACE FLOW ACROSS AN ELEVATION
GRADIENT ON THE COLORADO FRONT RANGE

Submitted by

Caroline Martin

Department of Ecosystem Science and Sustainability

In partial fulfillment of the requirements

For the Degree of Master of Science

Colorado State University

Fort Collins, Colorado

Spring 2018

Master's Committee:

Advisor: Stephanie Kampf

Sara Rathburn

Michael Falkowski

Copyright by Caroline Elizabeth Martin 2018

All Rights Reserved

ABSTRACT

SPATIAL AND TEMPORAL VARIABILITY IN CHANNEL SURFACE FLOW ACROSS AN ELEVATION GRADIENT ON COLORADO FRONT RANGE

Topographic indices such as Upslope Accumulation Area (UAA) and the Topographic Wetness Index (TWI) are commonly used in watershed analyses to derive channel networks. These indices work well for large rivers and streams, but they do not always produce stream locations that match those observed in the field for headwater streams, where geology and soils affect locations of surface channels. This study maps the actively flowing drainage network of four headwater watersheds across an elevation gradient in the Colorado Front Range and examines how these locations of flow relate to topography, geology, climate, and soils. The objectives are to 1) document and digitize the active stream networks in the field, 2) delineate stream network with topographic indices and evaluate how index-derived channel networks compare with observations, and 3) evaluate how geology, climate, and soils affect surface water flow paths. Study sites are small headwater watersheds (1.7 – 15.5 km²) that vary in elevation from 1780 m up to 4190 m. At each watershed, surveys of surface water locations were conducted twice during the summer about a month apart in order to capture temporal variation.

Stream densities documented during these surveys ranged from $5.09 * 10^{-4} \text{ m}^{-1}$ at highest elevation site (3494 m – 4192 m) to $1.83 * 10^{-3} \text{ m}^{-1}$ at lowest elevation site (1781 m – 2322 m). The lowest elevation site had the largest change in stream density between surveys, decreasing 84%. A middle elevation site that was affected by forest fire had the least change in stream

density with only a 5% decrease between visits. TWI and UAA methods for deriving channel networks from topography performed well relative to field observations, ranging from 73% to 91% accuracy at low and middle elevation sites. At high elevation sites, these methods had the poorest performance, with accuracy between 21% and 74%. Also, at high elevation sites TWI performed slightly better than UAA, with 6-25% increased overall accuracy. Comparing channel networks at the four catchments, stream densities generally decreased with elevation, whereas streamflow magnitude and duration increased with elevation. Although stream density decreased with elevation, it had no apparent relationship with precipitation.

The soil and bedrock geology were linked to streamflow location; in some cases, streamflow was discontinuous or dried up quickly in areas with high bedrock/soil hydraulic conductivity. Streams also followed shear zones, faults, and bedding contacts, where rocks are “weak”, whereas they diverted around less erodible pegmatites. Results suggest that topography is the primary factor controlling streamflow location; however, geology and soils explained some of the cases where topographic predictions of flow location were inaccurate. Future channel delineation methods could add in a parameter based on the hydraulic conductivities of underlying soil and bedrock to improve stream channel mapping.

ACKNOWLEDGEMENTS

What an experience it has been to research alongside wonderful professors and engaged students within the Watershed and Geology program. I am so thankful for the time I had at CSU and thankful for all those who contributed to my journey as a graduate student. First, I would like to thank all those who provided me discharge data for the 2016 water year which gave a foundation to my thesis; this list of contributors includes USGS, Boulder Critical Zone Observatory, John Hammond, and Codie Wilson. I, of course, would like to thank my advisor Stephanie whom I am beyond thankful for her time, teaching, feedback, and support; she always inspired me and encouraged me throughout the process of writing a thesis, which made it so much more delightful. I would also like to thank our lab group (John, Alyssa, Codie, Jason, Chenchen, Abby) and officemates (Beth and Tristan) for the nerdy comradery and creating a friendly environment that cultivated ideas, innovations, and intriguing research discussions that helped me grow as a scientist and kept me sane. A special thanks to my Geology girls: Kathryn, Kajal, Heather and Nikki, for always making things better and lifting my spirits. An enduring thanks to my family J., Diana, Trevor and Kelsey for always supporting me and loving me. Last but not least, I would like to thank Gabe for always believing in me and for joining me on insane field hikes, I couldn't have done it without him. (And even though he will never be able to read this, I would really like thank Mica, my dog, who joyfully went on almost all hikes and always cheered me up at the end of a long day at school).

TABLE OF CONTENTS

ABSTRACT ii

ACKNOWLEDGEMENTS iv

LIST OF TABLES viii

LIST OF FIGURES ix

1. INTRODUCTION 1

2. BACKGROUND 3

 2.1. Intermittent streams 3

 2.2. Hydrography data 4

 2.3. Controls on channel initiation and stream locations 4

 2.3.1. Topographic indices and channel delineation 4

 2.3.2. Environmental variables 8

 2.4. Study Sites 10

 2.4.1. Mountainous catchments 10

 2.4.2. Lower (L): Mill Creek 14

 2.4.3. Middle Burned (MB): Skin Gulch 16

 2.4.4. Middle Unburned (MU): Gordon Creek 18

 2.4.5. Upper (U): Andrews Creek 20

3. METHODS.....	22
3.1. Field work.....	22
3.2. Topography	23
3.2.1. DEM acquisition and topographic analysis (UAA and TWI).....	23
3.2.2. Evaluation metrics	26
3.3. Environmental variables.....	28
4. RESULTS.....	29
4.1. Observed channel networks	29
4.2. Topographic thresholds for deriving channel networks	33
4.3. Accuracy of derived channel networks	37
4.4. Catchment comparisons	44
4.5. Physical catchment characteristics affecting stream networks.....	49
4.5.1. Geology.....	50
4.5.2. Soils.....	52
4.5.3. Vegetation and Aspect	52
5. DISCUSSION.....	54
5.1. Lower (L).....	54
5.2. Middle burned (MB).....	57
5.3. Middle unburned (MU)	59

5.4. Upper (U).....	62
5.5. Topography	63
5.6. Vegetation and Aspect	70
5.7. The overarching effects of climate/elevation	71
5.8. Landscape evolution.....	73
5.9 Uncertainties	73
5.10 Conceptual Model and Future Considerations	74
6. CONCLUSIONS	78
REFERENCES	80

LIST OF TABLES

Table 1: Summary of study site characteristics 13

Table 2. Dates for field mapping of stream networks in 2016 22

Table 3. Characteristics of the stream network and streamflow of the study sites for water year 2016 and for Trip 1 and Trip 2 30

Table 4. Threshold values of A, $\ln(a)$, and TWI for Trips 1 and 2 with 10 m and 1 m DEMs 35

Table 5. The difference of $\ln(a)$ and TWI from Trip 1 and Trip 2, where the values in the table represent $\ln(\tan\beta)$ 36

Table 6. Accuracy assessment of the derived channels compared to observed channels. FP is the % false positive and FN is % false negative. % Accuracy is the total % of the derived network length that is correct..... 41

Table 7. Quantitative results showing the number of stream tributaries during each trip (#) for observed and derived channel ($\ln(a)$ and TWI) networks 43

LIST OF FIGURES

Figure 1. Locations of study catchments in north central Colorado. Left: National Geographic World Map (ESRI), Right: World Imagery (ESRI). 11

Figure 2. Study catchments over (a) elevation (U.S. Geological Survey, 1991), and (b) mean annual precipitation (PRISM Climate Group, 2017). 12

Figure 3. Catchment characteristics of Lower (L, Mill Creek) with the field map stream flow from trip 1 in early June..... 15

Figure 4. Catchment characteristics of the middle burned (MB, Skin Gulch) catchment with the field-mapped stream flow from trip 1 in late June..... 17

Figure 5. Catchment characteristics of Gordon Gulch with the field-mapped stream flow from trip 1 during mid July 19

Figure 6. Catchment characteristics of Andrews Creek (U) with the field-mapped stream flow from trip 1 21

Figure 7. 3x3 roving window with cells alphabetized. ‘e’ is the target cell, while ‘a’, ‘b’, ‘c’, ‘d’, ‘f’, ‘g’, ‘h’, and ‘i’ are the neighboring cells..... 24

Figure 8. Conceptual diagram of flow accumulation algorithm 25

Figure 9. Visualization of evaluation metrics used in this study 27

Figure 10. Field mapped stream networks from trip 1 and trip 2 (left) and hydrographs for WY2016 indicating when trip 1 and trip 2 were conducted (right)..... 33

Figure 11. Changes in channel length and stream density (lines) for varying values of 10 m ln(a) and TWI thresholds for each watershed	34
Figure 12. First Trip observed stream network (blue) compared with the first trip flow 10 m accumulation threshold (pink), 10 m TWI threshold (green), and NHD High Resolution network (brown).....	38
Figure 14. Mean elevation relationships with stream density (a), days of flow (b), discharge (c), and number of channel heads (d).....	45
Figure 15. Annual 2016 precipitation relationships with a) stream density, b) days of flow, c) discharge, and d) number of channel heads	46
Figure 16. Variation in TWI thresholds for each watershed and trip with climate factors and watershed characteristics.....	48
Figure 17. Comparison of elevation and climate variables and their effect on stream density. .	49
Figure 18. Geologic maps of all sites highlighting connections between geology and stream locations.....	51
Figure 19. Hydraulic conductivities, K, for different rock types (Heath, 1983)	56
Figure 20. MB's (Skin Gulch) channel bed that is wide, armored with coarse sediments, and includes segments of exposed bedrock.....	57
Figure 21. Example of other streams near MB (Skin Gulch) that had streams that followed shear zones and faults.	58

Figure 22. Summer rain events led to flow in Gordon Creek (MU) during August and September
..... 59

Figure 23. An example of a log jam at MU where water was dammed behind the log and
resurfaced a meter downstream from the log jam 61

Figure 24. Flat open area along MU (Gordon) channel valley is dry. 62

Figure 25. Total % accuracy of each 10 m topographic index for mapping surface flow locations
at every study site..... 64

Figure 26. Resolution of DEMs (10 m or 1 m) and GPS mapped stream (5-8m) 68

Figure 27. Linear relationship between $\ln(a)$ and stream density at the study catchments (left)
compared with Helmlinger et al. (1993) catchments from New York, California, and Idaho 69

Figure 28. Conceptual model showing the effects of relative hydraulic conductivity on surface
channel flow depending on the magnitude of flow. 75

Figure 29. Conceptual model showing the effects of bedrock hydraulic conductivity and
structural geology on streamflow location..... 76

1. INTRODUCTION

Headwater stream networks are complex systems, where the location and amount of surface flow changes in space and time. Topography, soils, geology, vegetation, and climate all affect how water moves through its landscape. These variables vary within a catchment and between catchments making it difficult to understand how they interact to affect stream flow patterns. Topography has been linked to spatial runoff patterns in a catchment (Beven and Kirkby, 1979; Woods et al., 1997), with streams typically found in areas with high contributing area and topographic convergence (Dunne and Black, 1970; Anderson and Burt, 1978; Beven, 1987; Savenije, 2010). Locations of small headwater streams can also be influenced by geology, soil, and vegetation (Jensco and McGlynn, 2011; Emanuel et al., 2014; Villines et al., 2015; Wagener et al., 2007). Extensive research has been devoted to the use of Digital Elevation Models (DEMs) in hydrological analysis because topographic attributes such as slope, upslope area, curvature, and openness can be derived from DEMs and used in channel delineation. While many applications use channel networks derived from DEMs, these derived networks are not always accurate (Helmlinger et al., 1993; Jaegar et al., 2007; Orlandi et al., 2011), and a better understanding of how other catchment attributes affect the stream network could improve future models. The questions motivating this research are (1) can topographically derived channel networks represent spatial patterns in surface flow?, and (2) what other physical factors affect stream location? The research objectives to address these questions are to (1) determine where and when surface streams are flowing in small headwater catchments across

an elevation gradient; (2) evaluate how field mapped streams compare to those derived from surface topography; and, 3) assess how other physical attributes (geology, soil, vegetation, aspect, climate) relate to stream flow patterns.

2. BACKGROUND

2.1. Intermittent streams

Headwater streams are dynamic, expanding and contracting seasonally and/or annually. Parts of the channel network that do not flow continuously in time are called intermittent, and these streams make up 50-70% of stream length in the US (Datry, 2014; Nadeau and Rains, 2007). Godsey (2014) mentions that anyone who spends sufficient time in a headwater catchment will observe that channel networks are rarely fixed features of the landscape. These types of spatially and temporally transient streams are often classified as intermittent or ephemeral streams. Intermittent streams have flow for part of the year (usually seasonally) unlike perennial streams that flow year-round. Ephemeral streams flow only following storm events. These streams are intrinsic to the ecological and biochemical functions and to the biodiversity of river systems (Stanley et al., 1997; Fisher et al., 2004; Meyer et al. 2007; Dodds and Oakes, 2006, 2008; McIntyre et al., 2009). Any changes in the timing of the drying and wetting or in the spatial connectivity of streamflow directly affect the aquatic biota and could result in periods of habitat loss (Jaeger et al., 2012; Cote et al., 2009). Although intermittent streams may receive no flow for substantial portions of a year, they can still strongly influence downstream water quality and are essential to groundwater recharge (Niswonger et al., 2005; Goodrich et al., 2004; Dowman et al., 2003; Morin et al., 2009; Villeneuve et al., 2015).

2.2. Hydrography data

Researchers typically rely on public hydrography data for mapping stream networks in an area, and these networks are then used in models quantifying water fluxes, water quality, or landscape evolution. The National Hydrography Dataset (NHD) (U.S. Geological Survey, 2013) is a publicly available river network dataset maintained by the USGS, and it was created to assist scientists and land managers in modeling hydrologic features, water quantity, and water quality. There are many versions of NHD, as the dataset is updated to improve the resolution or add more reach file information. NHD High Resolution was derived from the USGS Digital Line Graph at a scale of 1:24,000 and combined with the EPA reach files version 3.0 (RF3), which supplies the reach-scale attribute data. NHD High Resolution offers a horizontal accuracy of 0.02 inch on map scale, which is 12 m at the scale of 1:24,000. Some studies have used NHD data as a reference for the true river network (e.g., Di Luzio et al., 2002, Li and Wong, 2010). However, many other studies have found that NHD is inadequate at mapping headwater streams, and in some cases it may underestimate the extent of intermittent and perennial streams (e.g. Hansen, 2001; Paybins, 2003; Childers et al., 2006; Fritz et al., 2013, Villines et al., 2015). Improved understanding of the controls on stream flow location would help to improve the accuracy of current hydrography data.

2.3. Controls on channel initiation and stream locations

2.3.1. Topographic indices and channel delineation

Channel delineation methods using topographic data were first created in geomorphic studies that were simulating erosion (Moultrie, 1970; Sprunt, 1972). Later studies developed methods

deriving topographic attributes from Digital Elevation Models (DEMs) to delineate channels.

The primary topographic attributes used in these algorithms are surface slope, upslope area, curvature, openness, or combinations of these attributes. Upslope accumulation area (UAA) (Helmlinger et al., 1993; Gallant et al., 1996; Jenson and Dominique, 1988; O'Callaghan and Mark, 1984; Omran, 2016; Erskine et al., 2006) and the topographic wetness index (TWI) (Beven and Kirkby, 1979; Beven and Wood, 1983; Beven and Freer, 2001; Qin et al., 2011; Quinn et al., 1995; Sørensen, 2006) are the most commonly indices used to delineate channels.

Upslope Accumulation Area (UAA) is the area that drains into a single point (or grid cell) along a stream. This term is synonymous with contributing area, upslope area, drainage area, source area, and flow accumulation, and it represents the area that can potentially contribute runoff to a given location. UAA can be determined via a flow routing algorithm, which determines the paths of water through a landscape. Many algorithms have been created to route flow and to fill depressions or pits in the DEM data. The first and most foundational flow direction method created was the D8, which assigns flow from each pixel to one of its eight neighbors in the direction with the greatest downward slope (O'Callaghan and Mark, 1984). Researchers found that this did not work well in areas with low slope, so other algorithms were created to allow water to move into more than one neighboring cell. Such algorithms include but are not limited to the following: Multiple direction algorithm (MF) (Quinn et al., 1991); Lea's method (1992), DEMON (Costa-Cabral and Burges, 1994), Dinf (Tarboton, 1997), D8 LAD and D8 LTD (Orlandini et al., 2003) and Rueda's MF method (2013). While such methods may improve channel network mapping in some locations, McMaster (2002) and Hastings (2012) saw no benefits for

network accuracy in steep terrain as a result of using D^∞ versus D8. Other modifications to the flow direction algorithm have improved the depression filling step (Jensen and Domingue (1988); Martz and Garbrecht, 1998; Lindsay and Creed, 2005a, b).

The topographic wetness index (TWI) is a commonly used topographic index that was developed to indicate spatial patterns of saturated areas. TWI is the natural log of UAA over cell length divided by the tangent of local slope ($\ln[(UAA/L)/\tan\beta]$). This index has been compared to many spatial variables including soil moisture distribution (Western et al., 1999), soil type, soil organic matter distribution (Pei et al., 2010), vascular plant species richness (Zinko et al., 2005), groundwater level (Kaser et al., 2014), hydrological processes (Tarboton, 1991, 1992; Sørensen, 2006), and stream water quality. Some authors suggest that any moisture related, spatially distributed state variable of a catchment can be correlated with or derived from topographic wetness indices (Grabs et al., 2009).

Channels can be defined from UAA or TWI based on threshold values, which have been called channel threshold area (CTA), channel initiation threshold (CIT), or optimal threshold area. These threshold values define the Upslope Accumulation Area and TWI value needed to initiate flow. Users select a threshold value to reduce the excessive length of the stream network produced by DEMs and to match observed stream networks (Tarboton et al., 1991, 1992; Benstead and Leigh, 2012). The values of the thresholds can vary considerably for different locations and applications (Helmlinger et al., 1993; Heine, 2004; Clubb et al., 2014) and for different DEM resolutions (Zhang and Montgomery, 1994; Wolock and McCabe, 2000;

McMaster 2002; Utery et al., 2004; Kienzle, 2004; Sørensen and Seibert, 2007; Colson et al., 2008; Vaze et al., 2010; Hastings and Kampf, 2014). The chosen threshold should avoid overestimating the channel network and should reflect the local landscape (Fotheringham, 1997). Many methods of choosing a threshold have been tested, but none have been completely successful. One common method is trial and error, which compares the visual similarity between the extracted network and the lines depicted on the topographic maps. Another popular method is using a slope-area relationship (Montgomery et al., 1993; O'Callaghan and Mark, 1984). A slope-area relationship is thought to represent the different geomorphic processes and specifically the hillslope/valley transition that can be used for identifying channel heads. However, in many studies this has not worked well due to subsurface controls on channel initiation (Jaegar et al., 2007; Orlandini et al., 2011; Hastings, 2012). Other methods include using 1% of the maximum flow accumulation, the first break value from standard deviation, or a multifractal analysis for determining an optimal threshold value (Band, 1986; Deilami et al., 2013; Tarboton, 2005).

Investigations of DEM resolution on various terrain indices have found that different grid resolutions lead to different terrain index values (Zhang and Montgomery, 1994; Wolock and McCabe, 2000; McMaster 2002; Utery et al., 2004; Kienzle, 2004; Sørensen and Seibert, 2007; Colson et al., 2008; Vaze et al., 2010; Hastings and Kampf, 2014). Most researchers agree that using a DEM resolution between 1 m and 10 m gives the most accurate representation of the topography because it captures fine-scale topographic features; some researchers have found

that 10 m is better for channel delineation because groundwater is less likely to follow microtopography (Jensco et al., 2009; Grabs et al., 2009).

While many studies have compared derived channel networks with different flow routing algorithms (Gallant et al., 1996; Orlandini et al., 2003; Qin et al., 2011; Rueda et al., 2013; Sørensen et al., 2006) or using various DEM size or topographic indices (Sørensen and Seibert, 2007; Vaze et al., 2010; Hastings 2012), few have compared derived networks to field maps of surface flow locations. The lack of field data limits the ability to evaluate the derived channel networks, but this comparison is critical for improving the accuracy of derived stream channels. Only a few studies out of the hundreds on topographic channel delineation have used observed channel heads and stream networks to evaluate their derived channel networks (e.g. Montgomery and Dietrich, 1989; Jaeger et al., 2007; Güntner et al., 2004; Priotti et al. 2010; Sofia et al. 2011; Jensco and McGlynn, 2011; Clubb et al., 2014; Russell et al., 2015; Villines et al., 2015). Others have used NHD or other publicly available stream networks as a true river network reference (e.g., Di Luzio, Srinivasan, & Arnold, 2002d, Li and Wong, 2010); however, NHD is not always an accurate representation of headwaters and temporary streams (Hansen, 2001; Paybins, 2003; Childers et al., 2006; Fritz et al. 2013, Villines et al., 2015) and should not be used as a true reference.

2.3.2. Environmental variables

Surface topography reflects the combined influences of climate, geology, soils, and vegetation. Climate affects vegetation type, weathering rates, soil depth, and frequency of runoff

generation. Geology modifies runoff mechanisms (Onda et al., 2006; Jensco and McGlynn, 2011), flow regimes (Tague and Grant, 2004), flood time scales (Ladislav Gaa'l et al., 2012), vegetation density (Emanuel et al., 2014), and hydrologic connectivity (Jensco et al., 2009; Nippgen et al., 2011; Huff et al., 1982; Wolock et al., 1997; Burns et al., 1998; Onda et al., 2001, 2006). Soil can further influence the timing of a hydrologic response, hydrologic connectivity, and the storage capacity of a catchment (McNamara et al., 2005; Nippgen et al., 2011; Ali et al., 2014; Villines et al., 2015; Kelleher 2015; Kim and Mohanty, 2017). On a landscape scale, soil moisture patterns also affect runoff generation (Barling et al., 1994; Beven and Freer, 2001; Western et al., 1999; Yimer et al., 2006; Kampf et al., 2015).

Vegetation affects all scales of the hydrologic processes in a catchment (Emanuel et al., 2014). On a fine-scale, vegetation can alter the soil water balance by taking up water and intercepting precipitation (Rodriguez-Iturbe, 2000), whereas on a coarser scale vegetation type and density influences water yield and hillslope dynamics (Bosch and Hewlett, 1982; Jensco and McGlynn, 2011; Emanuel et al., 2014;). Some researchers have included environmental factors such as climate, vegetation, geology and soils (Villines et al., 2015; Vogt et al., 2003; Russel et al., 2015) in their channel derivation models, but soil, vegetation, and geology data may be too coarse to incorporate into channel derivation methods (Russel et al., 2015).

In steep mountain regions like my study area in the Colorado Front Range, soil depth is often relatively small due to steep slopes and low weathering rates. This may increase the importance of bedrock geology relative to soil in determining stream patterns. Slope aspect can also be

important for streams because it creates “microclimates” on varying hillslopes, which can alter evapotranspiration rates, water availability, soil properties, temperature, vegetation types, and snowpack dynamics (Bale et al., 1998; Yimer et al., 2006; Kelley, 2012; Hinckley et al., 2014).

2.4. Study Sites

2.4.1. Mountainous catchments

The study region is the Colorado Front Range of the Rocky Mountains, which has a large elevation range that leads to a gradient in climate, vegetation, and hydrologic processes (Figure 1, 2). Elevation is highly correlated to precipitation, temperature, and snow persistence (Richer et al., 2013). High elevations have cooler temperatures and higher precipitation, which leads to greater snow accumulation than at lower elevations. Lower elevations are semi-arid with a mean annual precipitation (P) over potential evapotranspiration (PET) < 0.5 (Middleton and Thomas, 1997). Most winter storms move west to east across the Rocky Mountains, and occasionally fast-moving storms from Canada move south and create significant snow fall (Doesken and Judson, 1996). Spring storms can also occur where moist air is lifted up the east upslope, creating an orographic effect, which results in snowfall or rain at the high elevations (Barry, 2008).

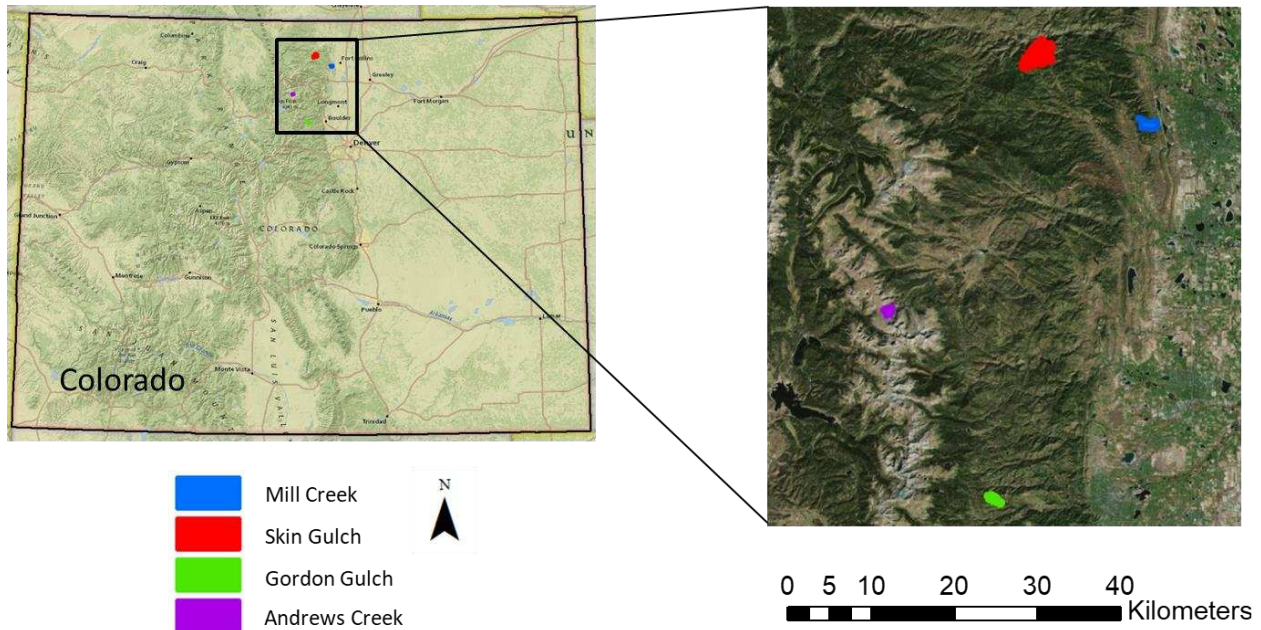


Figure 1. Locations of study catchments in north central Colorado. Left: National Geographic World Map (ESRI), Right: World Imagery (ESRI).

At higher elevations (>3200 m) streamflow is sustained by snow melt, whereas elevations below 2300 m are rain-dominated and release higher flows during rain events (Jarrett, 1990; Kampf and Lefsky, 2016). Catchments between these elevations have a mix between snow and rain-dominated influences on streamflow. These zones of different hydrologic processes also have varying yearly snow patterns. Richer et al. (2013) have classified the yearly snow patterns into three groups based on snow persistence (SP), which is the percent of time that snow is present on the ground surface between the months of January and June. Elevations above 3050m form the persistent snow zone (PSZ), defined as SP greater than 75% (Richer et al., 2013). The transitional snow zone (TSZ) is defined as SP between 50% - 75% and is found between 3050m – 2550 m; below this, snow is within the intermittent snow zone, not typically lasting continuously through the winter (25-50% SP) (Richer et al., 2013).

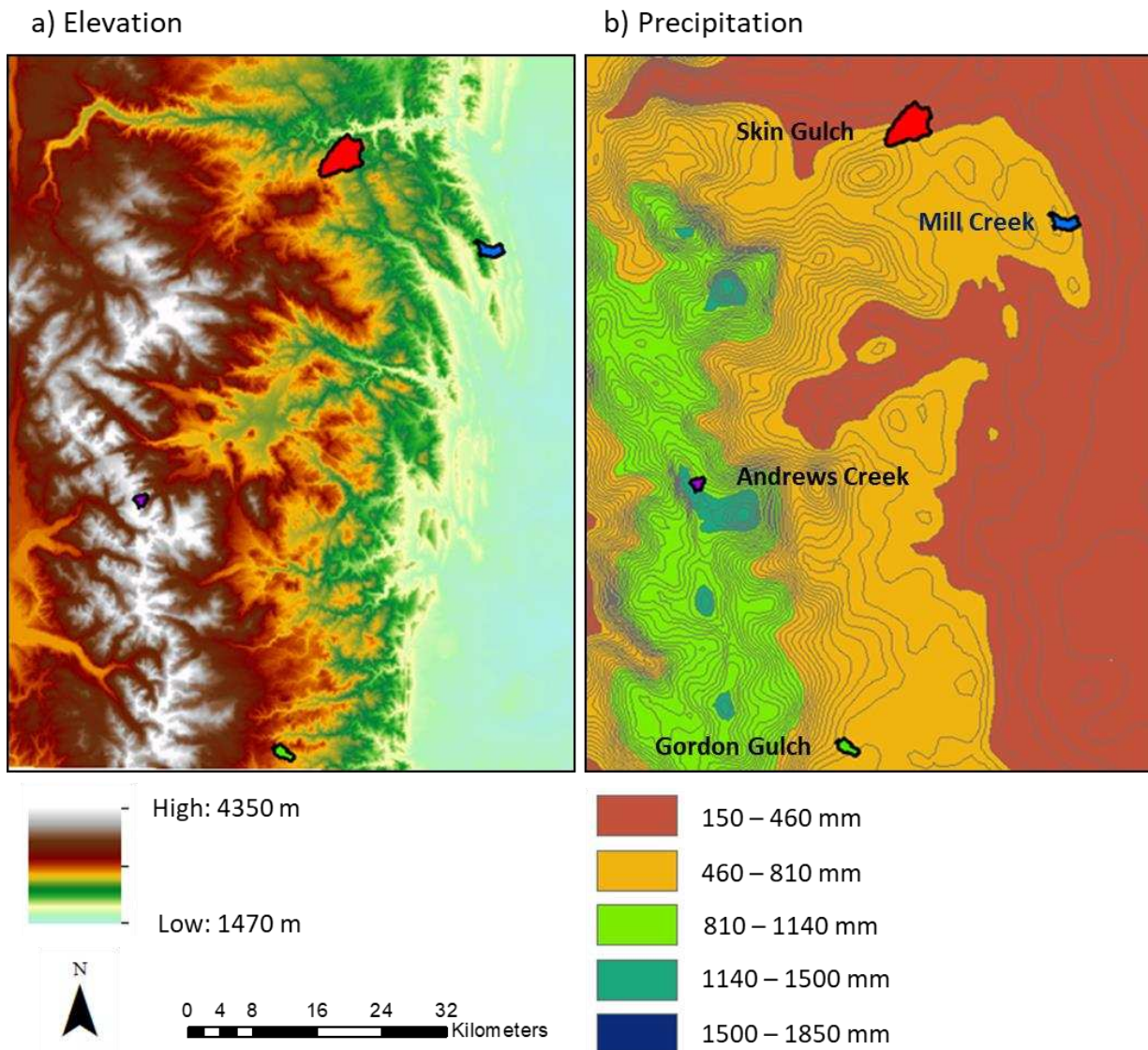


Figure 2. Study catchments over (a) elevation (U.S. Geological Survey, 1991), and (b) mean annual precipitation (PRISM Climate Group, 2017).

For this study, four small catchments (1.7km² to 15.5km²) were selected based on accessibility, availability of flow stage height or discharge data, and elevation so that they would span a gradient in climate (Figure 2). The lowest elevation site (L) is in the intermittent snow zone; middle elevation sites (MB, MU) are in intermittent and transitional snow zones, and the high

elevation site (U) is in the persistent snow zone. A burned intermediate site, MB, was added to examine the effects of fire on flow duration of an intermittent stream. Measurements were conducted in 2016, which was an average water year in which annual precipitation only varied about 10% from the 30-year normal annual precipitation. L had about the same annual P as the 30-year normal; MB and U had lower than normal annual P, and MU had higher than normal annual P. Table 1 summarizes the characteristics of the watersheds.

Table 1: Summary of study site characteristics.

Site Characteristics		Mill (L)	Skin (MB)	Gordon (MU)	Andrews (U)
Drainage area (km ²)		3.8	15.5	2.6	1.7
Elevation (m)	Range	1781 - 2322	1991 - 2877	2618 - 2926	3494 - 4192
	Mean	2039	2447	2818	3791
Slope (degrees)	Range	0.02 - 70.9	0 - 70.5	0.04 - 45.8	0.12 - 76.3
	Mean	21.5	22.3	13.9	37.1
Annual 30-yr normal P (mm) ¹		464	516	511	1292
2016 annual P (mm) ¹		471	468	560	1128
Dominant geology ²		Quartzo-feldspathic mica schist	Mica schist and Amphibolite	Gneiss	Talus and Granite
Dominant soil texture ³		Sandy loam	Sandy loam	Sandy loam	Rock outcrop and Talus
Climate Zone ⁴		Intermittent Snow Zone	Intermittent Snow Zone and Transitional Snow Zone	Transitional Snow Zone	Persistent Snow Zone
Snow Persistence (%) 2016 average ⁵		35	48	62	96

¹PRISM Climate Group (2017), ²USGS National Geologic Map Database (2016), ³Web Soil Survey (2017), ⁴Richer et al., (2013), ⁵Hammond et al., (2017)

2.4.2. Lower (L): Mill Creek

Mill Creek (L - lower) is the lowest elevation watershed in the foothills on the eastern slope of the Colorado Rocky Mountains (Figure 3). L is located within Lory State Park and drains into Horsetooth Reservoir, which is directly west of Fort Collins, Colorado. The watershed area is 3.78 km² with an elevation range of 1781 - 2322 m. The slope average is 21° and ranges from 0° - 62°. The steepest areas are mostly along bedrock outcrops bounding the creek. The resistant steep bedrock consists of mostly quartzofeldspathic mica schist (Braddock et al., 1989). Bedrock in the watershed also includes pegmatite and trondhjemite and toward the outlet a conglomerate where the slope is below 10°. Soil on the slopes are mainly a loamy-skeletal, mixed Lithic Eutroboralfs (Alfisols) with very high runoff (Soil Survey Staff, 2017). On the gentle slopes near the outlet is a well-drained fine-loamy mixed, Aridic Argiustolls (Mollisol) with high runoff. Alfisol is a soil suborder that is slightly acidic with clay-enriched B horizon, and Mollisol is a soil rich with mineral nutrients that has a topsoil with high organic matter content.

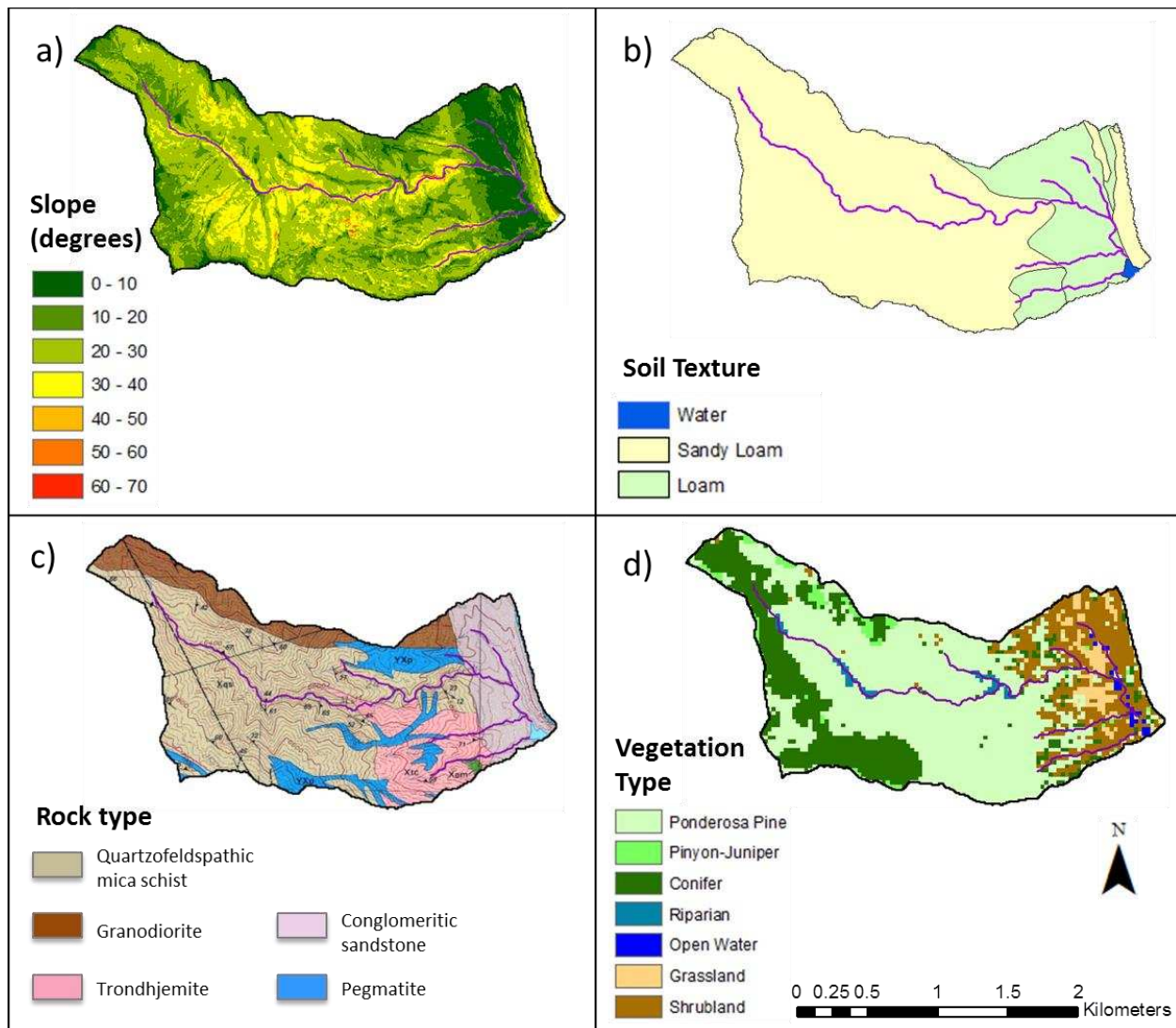


Figure 3. Catchment characteristics of Lower (L, Mill Creek) with the field map stream flow from trip 1 in early June. a) slope in degrees, b) soil texture (Soil Survey Staff, 2016), c) geology (Braddock et al., 1989), d) vegetation (Homer et al., 2015).

Climate in this watershed is semi-arid, and precipitation averages 464 mm per year. In 2016 total precipitation was 471 mm (PRISM Climate Group, 2017). Mean annual temperature over a 30-year normal is 47 °C, and during 2016, the mean annual temperature was 49.1 °C (PRISM Climate Group, 2017). L is within the Intermittent Snow Zone (ISZ). The watershed has a variety of vegetation types including grass and shrubs in the lower elevations and conifer forest in the

higher elevations. The main channel is an intermittent stream that flows mainly during winter, spring, and early summer.

2.4.3. Middle Burned (MB): Skin Gulch

Skin Gulch (MB – middle burned) is a burned watershed in the Front Range of that drains into the Cache la Poudre River (Figure 4). It is about 25 miles northwest of Fort Collins. MB is the largest of the study catchments with a drainage area of 15.5 km² and an elevation range of 1991 m to 2877m. The average slope is 22.3° but has a wide range from 0° to 70.5°. The geology of MB is very complex containing many metamorphic and igneous rocks such as amphibolite, augen mica schist, granodiorite, and pegmatite (Nesse and Braddock, 1989). This area is also structurally diverse including a shear zone running northeast to southwest and the Stove Prairie fault that runs northwest to southeast (Nesse and Braddock, 1989). The soil is mainly the Redfeather sandy loam, which is a loamy-skeletal micaceous Inceptisol with medium runoff and somewhat excessively drained, and the Bullwark- Catamount family, which is a well-drained loamy-skeletal Alfisol.

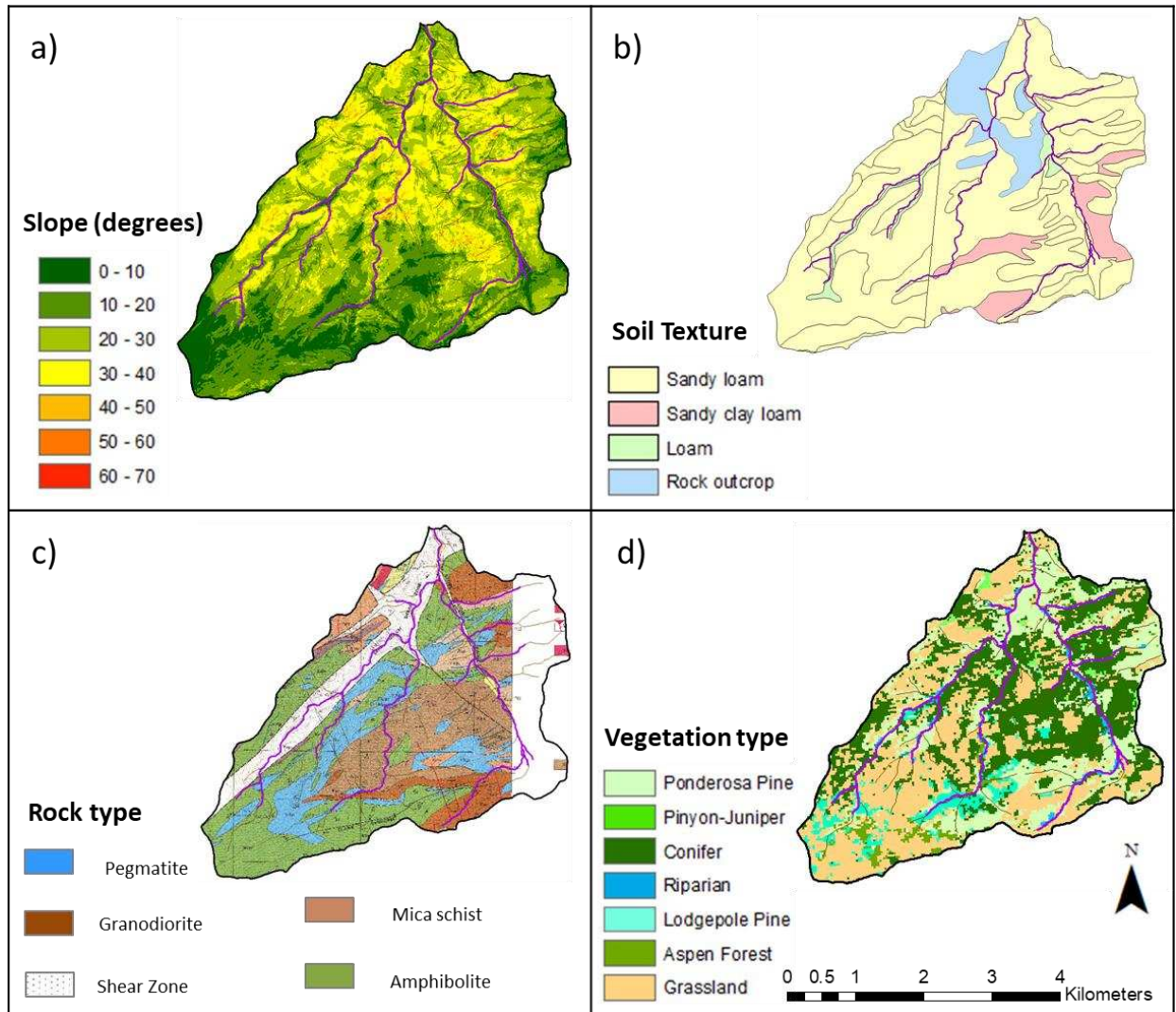


Figure 4. Catchment characteristics of the middle burned (MB, Skin Gulch) catchment with the field-mapped stream flow from trip 1 in late June. a) slope in degrees, b) soil texture (Soil Survey Staff, 2016) with two different surveys split the area in half, c) geology (Nesse and Braddock, 1989), d) vegetation (Homer et al., 2015) as mapped prior to the 2012 High Park Fire.

Climate is semiarid with a mean annual precipitation of 516 mm, and in 2016 precipitation was lower with 468 mm (PRISM Climate Group, 2017). Rain events are similar to those at the lower elevation site; in the summer these are usually convective storms, and occasional frontal storms occur in fall and spring (MacDonald and Stednick, 2003). Mean annual temperature over a 30-year normal is 44.1 °C, and during 2016, the mean annual temperature was 46 °C (PRISM

Climate Group, 2017). MB contains both the Intermittent Snow Zone (ISZ) and the Transitional Snow zone (TSZ) within its elevation range. Vegetation consists of forest, grass, and riparian upland shrubs (BAER, 2012). The forest types are predominantly lodgepole pine and ponderosa pine, with some douglas fir and aspen. These were mostly burned during the 2012 High Park Fire (BAER, 2012). Skin Gulch was burned primarily at moderate-high severity (65%), but the burn was mostly high severity in the higher elevation southern part (Kampf et al., 2016). In summer 2016, regrowth of understory was significant, but a majority of the dead trees were still standing. Dynamics of the watershed changed dramatically after the fire from a smaller intermittent stream pre-fire to a perennial stream with cobble bed and steep banks after the fire.

2.4.4. Middle Unburned (MU): Gordon Creek

Gordon Creek is an intermediate elevation site less than 20 miles west of Boulder (Figure 5). It is 2.64 km² and ranges from 2618 m to 2926 m in elevation. This watershed has relatively gentle slopes ranging from 0 to 45.74° and has an average slope of 13.94°. The geology is a cordierite-bearing sillimanite-biotite gneiss surrounding a quartz monzonite that runs mostly along the stream from northwest to southeast (Gable, 1980). Bedrock outcrops are common along the north side of the stream. Soil is mainly loamy-skeletal Inceptisols and Mollisols that have moderate runoff and are excessively drained with a sandy loam soil texture (Soil Survey Staff). Inceptisol is a young soil with horizons just beginning to develop and is typically found on weathering-resistant parent material or on high slopes. The climate is similar to that of L and MB, and on average it gets 511 mm of precipitation per year; in 2016 it had greater

precipitation with 560 mm (PRISM Climate Group, 2017). Mean annual temperature over a 30-year normal is 41.4 °C, and during 2016, the annual temperature was 44.2 °C (PRISM Climate Group, 2017). MU is within the transitional snow zone (TSZ). Most of the watershed is forested with lodgepole pine, ponderosa pine, some mixed conifer, and grass in the understory of ponderosa pine. Also, some riparian forest and woodland are found along the stream.

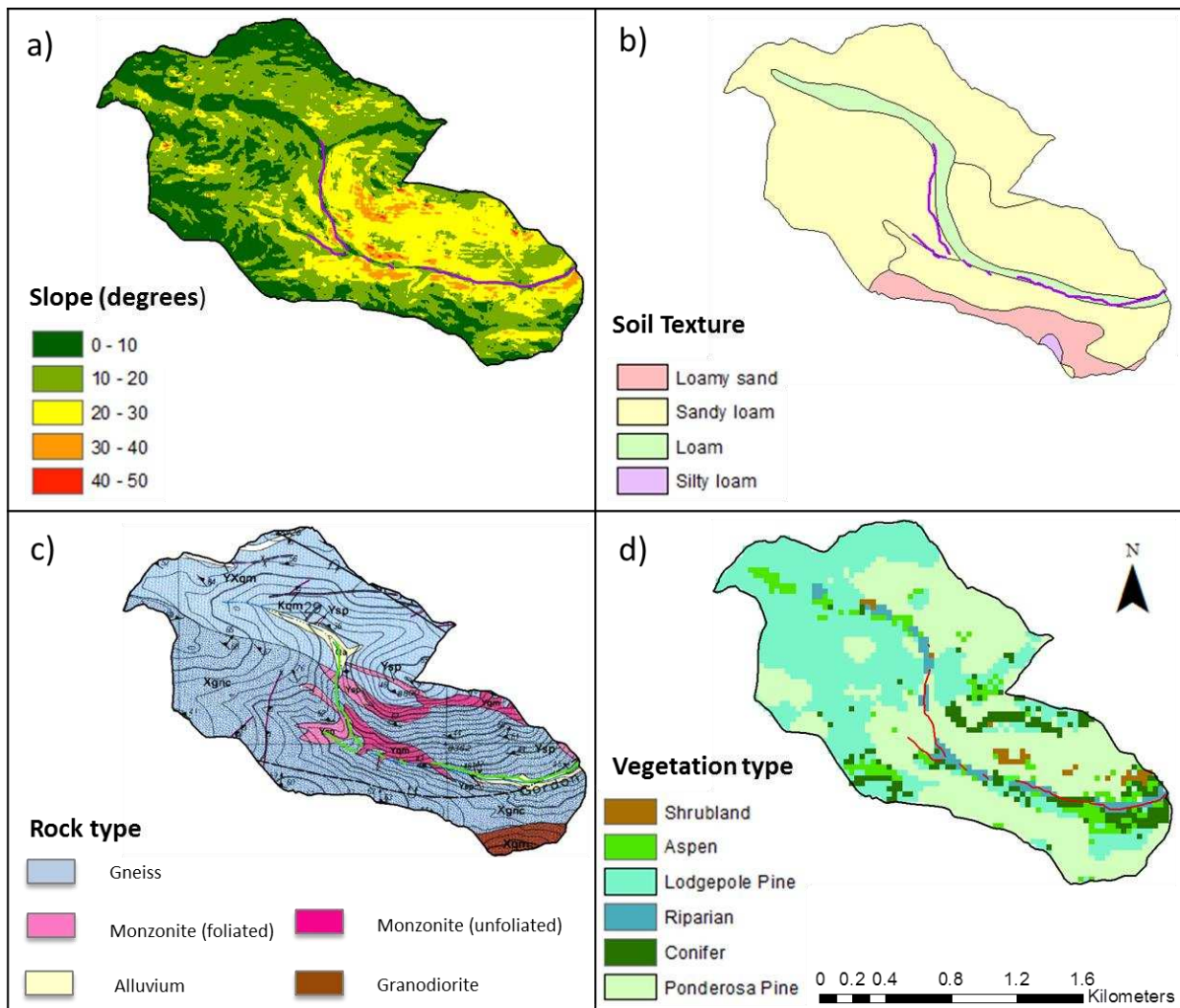


Figure 5. Catchment characteristics of Gordon Gulch with the field-mapped stream flow from trip 1 during mid July. a) slope in degrees, b) soil texture (Soil Survey Staff, 2016), c) geology (Gable, 1980), d) vegetation (Homer et al., 2015).

2.4.5. Upper (U): Andrews Creek

Andrews Creek (U- upper) is a 1.72 km² glaciated watershed within the Rocky Mountain National Park in Colorado (Figure 6). Its highest elevation is about 4192 m along the continental divide, and the lowest elevation is at the outlet at 3494 m within a meadow. The catchment was carved out by a glacier leaving a U-shaped basin and glacial till in its path. The sides of the basin are steep, and this can shade a large area of the watershed and therefore reduce direct sunlight. A small glacier called Andrew's Tarn remains at the Continental Divide, and at its base is a small lake from which the headwaters of U begin. 80% of the basin is bedrock and talus, where the bedrock is granite and granitic gneiss, which is composed of quartz, oligoclase, biotite, and microcline (Cole, 1977). The soil has a similar composition to the bedrock but with the addition of clays. Soil is only found on the gentle or near flat slopes in the meadow and is thin; otherwise the watershed is rock outcrop and rock debris. The thickness of soil ranges from 0.1 to 0.7 m and averages about 0.3 m (Soil Survey Staff, 2016). Near the meadow and outlet of U the soil is a loamy-skeletal Inceptisol with very high runoff and somewhat excessively drained.

The climate is that of a typical high elevation catchment in the Rocky Mountains of Colorado: summers are cool with frequent afternoon thunderstorms, and winters are cold and windy (Clow, 1996). Mean annual temperature over a 30-year normal is 29.2 °C, and during 2016, the mean annual temperature was 33.9 °C (PRISM Climate Group, 2017). Annual precipitation is about 1292 mm, and in 2016 it had lower precipitation with 1128 mm; snow during the winter and spring months makes up most of this precipitation (PRISM Climate Group, 2017). U is

within the persistent snow zone (PSZ). The growing season is only June, July and August when temperatures are warmer (Baron and Mast, 1992). Land cover is about 11% alpine vegetation such as forbs and grass and about 7% subalpine vegetation, which is old growth subalpine fir and Englemann spruce forest (Hartman et al., 1999).

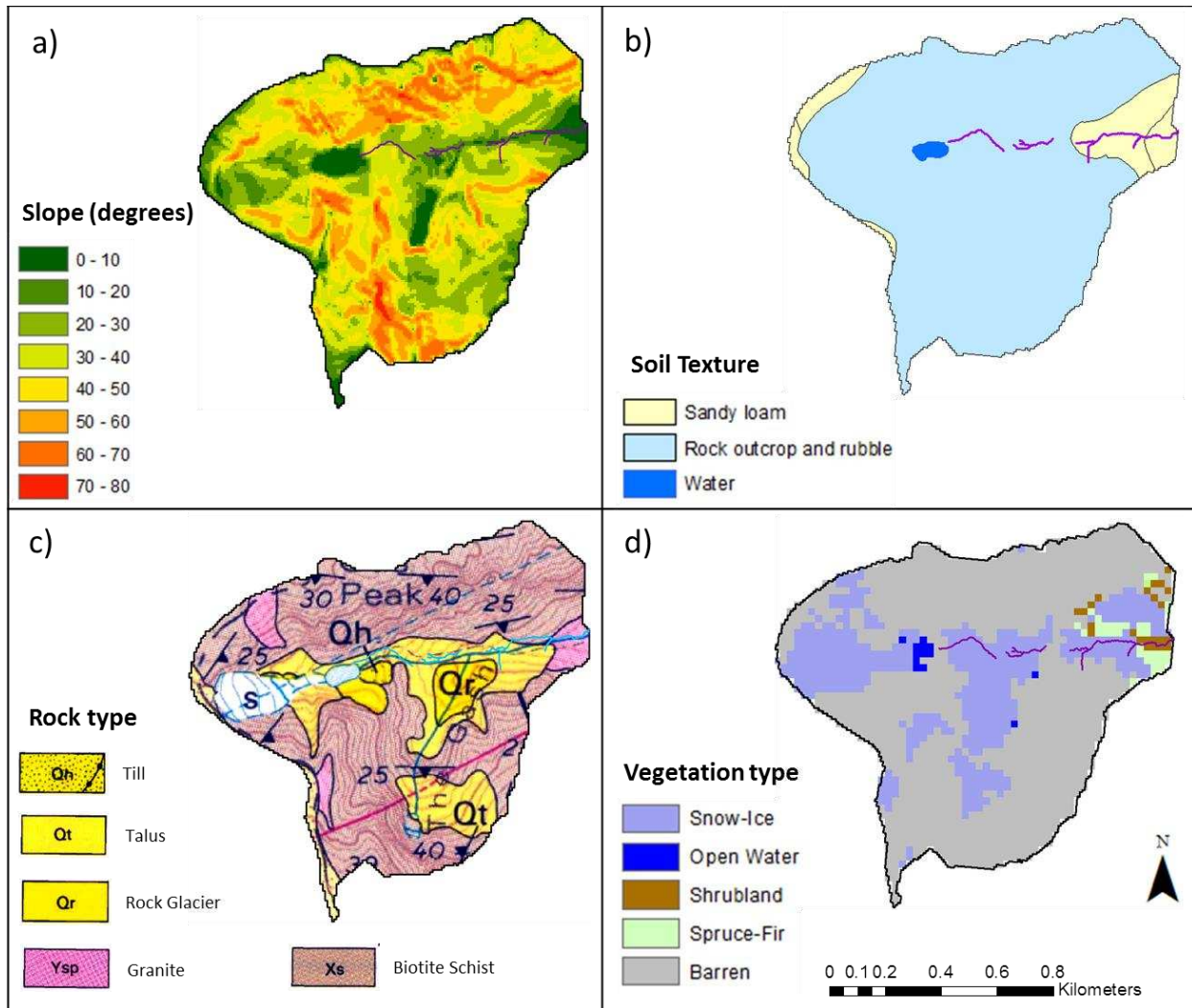


Figure 6. Catchment characteristics of Andrews Creek (U) with the field-mapped stream flow from trip 1. a) slope in degrees, b) soil type (Soil Survey Staff, 2016), c) geology (Braddock and Cole, 1990), d) vegetation (Homer et al., 2015).

3. METHODS

3.1. Field work

The stream networks of L, MB, MU and U were mapped twice during summer 2016 with intent to map at both high flow and low flow. Trip 1 was during June to mid-July, and trip 2 was mid-July to August. Table 2 shows specific trip dates for each site. For each watershed, surveys were completed within a week to avoid any large changes in the stream network during the survey. Mapping was conducted by plotting waypoints with a recreational GPS (Gaia GPS on a cellphone) and drawing the stream directly onto a topographic map. Recreational GPS was used for fast collection of data, as long distances had to be traversed. Also, the Gaia GPS has an accuracy of 5-8 m, which was sufficient to correspond with the resolution (10 m) of remote sensing data used in later methods. Gaia GPS allows offline navigation tools and uses the USGS topo map that can also be viewed as a basemap on ArcGIS; this allowed easy transferability of the waypoints to digitized stream networks in ArcGIS. The USGS topo maps have a scale of 1:24,000 and cover 7.5 minutes of longitude and 7.5 minutes of latitude.

Table 2. Dates for field mapping of stream networks in 2016.

Site	Trip 1	Trip 2
L	June 3-7	July 11-12
MB	June 24-30	August 10-15
MU	July 15-19	August 28-29
U	July 13	August 16-18

During each field visit I mapped the active network that contained visible flow and noted locations of headwaters and ponds. The active drainage network is different from the

geomorphic channel network, which is the branching network of topographic features that are diagnostic of erosion and deposition by channelized flows of water (Godsey, 2014). The stream densities (wetted stream length over drainage area) were then digitized on ArcGIS as line features, and the ponds were digitized as point features.

Discharge data were used to determine how long these streams flowed and where on the hydrograph the stream surveys were conducted. Discharge data was collected by various people and organizations: Mill Creek discharge was collected by John Hammond (CSU PhD candidate), Skin Gulch was collected by Codie Wilson (CSU PhD candidate), Gordon Gulch was collected by Boulder Creek Critical Zone Observatory (Anderson and Rock, 2016), and Andrew's Creek was collected from USGS. At each location, stage was measured using caprods or pressure transducers that logged data year-round, and then a stage-discharge rating curve was created based on manual discharge measurements. I computed area-normalized discharge for each location by dividing the discharge by the drainage area to facilitate comparison of the different sized catchments.

3.2. Topography

3.2.1. DEM acquisition and topographic analysis (UAA and TWI)

Next, I conducted topographic analyses to derive channel networks from digital elevation data using the watershed tools in ArcGIS. For this analysis, I used a flow accumulation algorithm (Fac) to determine flow directions and upslope areas (UAA), and I used these areas to compute the Topographic Wetness Index (TWI). Both operations can be calculated through ArcGIS (Arc

Hydro) with different focal operations. A focal function (neighborhood) is a spatial algorithm that uses a matrix to incorporate the neighboring cells into the calculation of each target cell. This 'matrix' is essentially a 'roving window' as it calculates an operation including neighboring cells (cells surrounding the target cell) over each target cell (i.e. e); the roving windows (matrix) can range in size (i.e. 3x3, 5x5, 9x9, etc.) but most commonly the 3 x 3 is used (Figure 7).

a	b	c
d	e	f
g	h	i

Figure 7. 3x3 roving window with cells alphabetized. 'e' is the target cell, while 'a', 'b', 'c', 'd', 'f', 'g', 'h', and 'i' are the neighboring cells.

Digital elevation model (DEM) data files are utilized as the input raster layer in both topographic algorithms. DEMs are a 3D representation of the earth's surface in the form of a raster. I used the USGS NED 1/3 arc-second, which is equal to a 10 m x 10 m resolution. For U and MU, I also obtained USGS 1/9 arc-second LiDAR (1 m resolution), and for L and MU, I used 1 m LiDAR DEMs from NEON (2013). I chose 1 m and 10 m DEMs rather than 30 m because Hastings (2012) found 10 m to be the best in deriving stream networks, and 1 m to give highly detailed topographic information that could provide a better information about geomorphological features. Also 30 m was found to be inadequate in deriving headwater channels in other studies (Montgomery and Foufoula-Georgiou, 1993; Hastings, 2012).

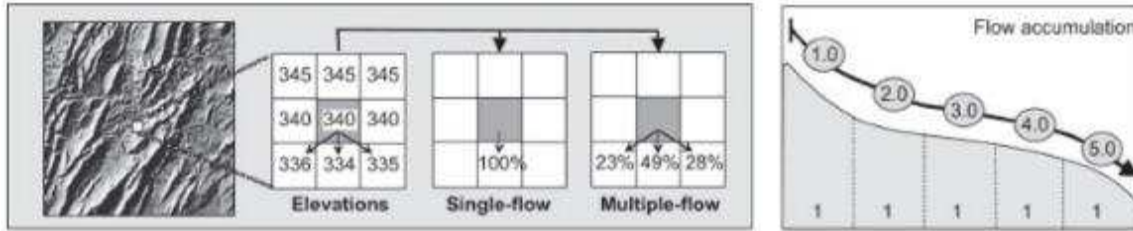


Figure 8. Conceptual diagram of flow accumulation algorithm. Left: flow accumulation operations weighted by single flow algorithms and multiple-flow algorithm. Right: example of unweighted flow accumulation along hillslope (Schäuble et al., 2008).

Using these DEMs I created flow direction rasters with the 'flow direction' tool in ArcGIS, which uses a single flow direction algorithm (D8) (Figure 8). I used the single flow direction algorithm (D8) because other studies have found that single-flow direction and multi-flow direction algorithms work equally well in deriving stream networks for steep landscapes (McMaster, 2002). From the flow direction grids, I calculated UAA using the 'flow accumulation' tool in ArcGIS and multiplied the resulting values (Fac) by the pixel area (L^2) (Equation 1). I compared the resulting flow accumulation maps using the 'fill' tool and not using 'fill' to determine which method best represented the observed stream. With the exception of U, stream flow patterns better matched flow accumulation with sinks filled.

$$UAA = Fac * L^2 \quad \text{(Equation 1)}$$

For TWI, I divided UAA by the length of a cell to create the specific contributing area, 'a', (Equation 2), which is needed for the TWI calculation (Equation 4).

$$a = UAA/L \quad \text{(Equation 2)}$$

TWI is then computed as:

$$TWI = \frac{\ln(a)}{\ln(\tan\beta)} \quad \text{(Equation 3)}$$

$$TWI = \ln\left(\frac{a}{\tan\beta}\right)$$

(Equation 4)

Where 'a' is specific contributing area, and 'tanβ' is the local slope as percent rise. To facilitate comparisons between channel networks derived from UAA and TWI, I used the natural log of a (ln(a)) rather than UAA to define networks.

Thresholds for UAA and TWI were chosen to represent the upslope drainage area or TWI value at which streamflow initiates. To determine these threshold values, I iteratively tested different TWI and ln(a) thresholds and determined the total channel length for each. The threshold selected for each mapped stream network is the value for which the derived channel length was closest to the observed channel length. Thresholds were chosen for both UAA and ln(A), for both trips, and for both DEM sizes. To compensate for the 5-8m GPS accuracy error, I used an 8 m buffer on the field mapped stream to determine whether or not the derived channel networks overlapped with the field mapped networks.

3.2.2. Evaluation metrics

A variety of performance criteria were applied to evaluate the ability of the topographic indices and NHD (NHD High Resolution), to represent the spatial and temporal patterns of the observed stream networks. I utilized the most up to date NHD dataset, NHD High Resolution, which is the high resolution national hydrography dataset that is equivalent to NHD Plus V2 but without reach files. Potential errors in both NHD and the derived networks are: mapping tributaries that were not observed in the field (false positive), missing tributaries that were

observed in the field (false negative), and incorrect channel head placement (Figure 9). As used here, the term channel head is not the geomorphic channel head but rather the point of surface flow initiation (Montgomery and Dietrich, 1988). I documented the number of channel heads that were correctly identified by topographic indices as 'correct CH'. I computed false positive (FP) as the percent of the derived channel network length that is unobserved tributaries and false negative (FN) as the percent of the observed stream network length that is not represented by the derived stream network. FP was calculated by dividing the length of the derived stream that did not match the observed stream by the total length of the derived network and then multiplying by 100. FN was calculated by dividing the length of the observed stream network that did not match the derived stream network by the total length of the observed network and then multiplying by 100. I also computed the % accuracy as the length of the derived stream network that matches the observed stream network divided by the total length of the derived stream network times 100.

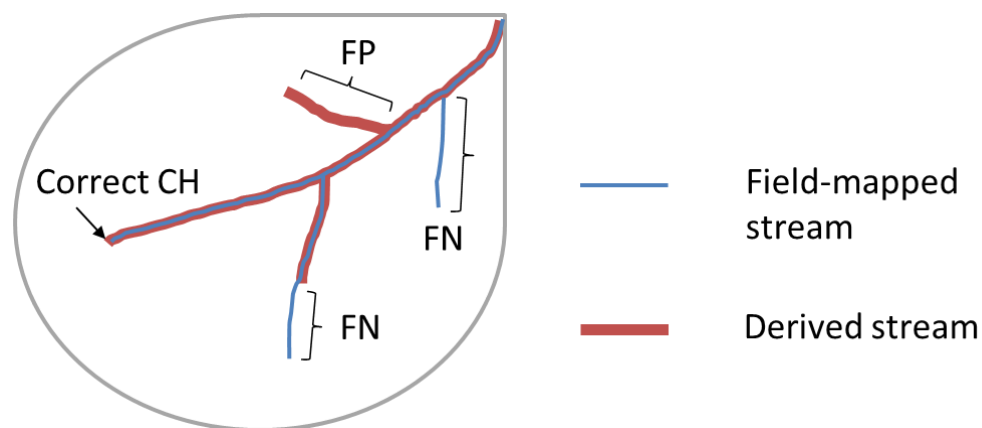


Figure 9. Visualization of evaluation metrics used in this study. Channel heads (CH) are the points of surface flow initiation; false positives (FP) are channel segments that were mapped by topographic algorithms but not observed in the field; false negatives (FN) are channel segments that were observed in the field but not mapped by the topographic algorithm.

3.3. Environmental variables

Next, I visually compared the field mapped stream networks from both trip 1 and 2 to geology, soil, vegetation, and aspect to determine the potential influences of these variables on stream location and duration. Geologic maps with a scale of 1:24,000 were acquired from the USGS National Geologic Map Database (2016). Soil textures were calculated from web soil survey data for each site (Soil Survey Staff, 2016); these maps range in scale from 1:12,000 to 1:63,360 where more details are gathered at 1:12,000 scaled maps (Soil Survey Staff, 2016). Vegetation type maps were from the National Land Cover Database (NLCD; Homer et al., 2015), which were in raster format and had a resolution of 30 m cells. It is important to note that the streams were small, usually about 1 m or less in width, so the scales of the datasets for environmental factors were typically coarser resolution than the streams, resulting in some uncertainty in the results. I also compared locations where TWI and $\ln(a)$ derived channels were incorrect (FP and FN), to the geology, soil, vegetation and aspect to determine if these factors could explain errors from topographically-derived channel networks.

4. RESULTS

4.1. Observed channel networks

The streams varied temporally and spatially over the course of the two summer surveys. All surveys were conducted during the hydrograph recession (Figure 10), and the second survey for each site was about a month after the first survey. Table 3 shows a summary of streamflow characteristics of each site during each survey.

L had the greatest change in stream length between surveys, decreasing from a stream length of 6,936 m to 1,127 m (Table 3). In the second trip (mid-July), only two first order streams remained flowing. This watershed had the greatest stream density of $1.83 \times 10^{-3} \text{ m}^{-1}$ during trip 1 and then decreased significantly to the smallest stream density of $2.98 \times 10^{-4} \text{ m}^{-1}$ during trip 2, when the number of channel heads decreased from 7 to 2. The discharge at the outlet of the main monitored channel ranged from 0 to 8.42 mm/d during the 2016 water year, with 1.22 mm/d during trip 1 and no flow during trip 2. Flow along the monitored main channel was observed for 204 days during the 2016 water year.

Table 3. Characteristics of the stream network and streamflow of the study sites for water year 2016 and for Trip 1 and Trip 2.

Streamflow Characteristics for WY 2016		L	MB	MU	U
discharge range (mm/d)		0 - 8.42	0.07 - 1.88	0-3.16	0.23 -18.52
discharge mean (mm/d)		1.13	0.29	0.29	2.64
days of flow		204	365	236	365
Trip 1	stream density (m ⁻¹)	1.83 x 10 ⁻³	1.29 x 10 ⁻³	7.27 x 10 ⁻⁴	5.09 x 10 ⁻⁴
	stream length (m)	6936	19965	1917	874
	disconnected length (m)	54	0	367	0
	number of channel heads	7	12	5	5
	discharge (mm/d)	1.22	0.42	0.02	6.88
Trip 2	stream density (m ⁻¹)	2.98 x 10 ⁻⁴	1.23 x 10 ⁻³	6.34 x 10 ⁻⁴	7.38 x 10 ⁻⁴
	stream length (m)	1127	19068	1672	1268
	disconnected length (m)	0	0	367	166
	number of channel heads	2	9	5	7
	discharge (mm/d)	0	0.15	0.01	3.86

MB had the greatest stream length of 19,965 m for trip 1 (late June) and only decreased by about 900m of stream length in the second trip (mid-August), which equates to only 5% of the stream length; this loss of stream length was due to drying of three small first order tributaries, resulting in the number of channel heads decreasing from 12 to 9 (Figure 10). MB had a stream density of $1.29 \times 10^{-3} \text{ m}^{-1}$ with a discharge of 0.42 mm/d during trip 1 and a stream density of $1.23 \times 10^{-3} \text{ m}^{-1}$ with a discharge of 0.15 mm/d for trip 2. MB flowed the whole year with an average discharge of 0.29 mm/day and had a discharge range of 0.07 to 1.88 mm/d.

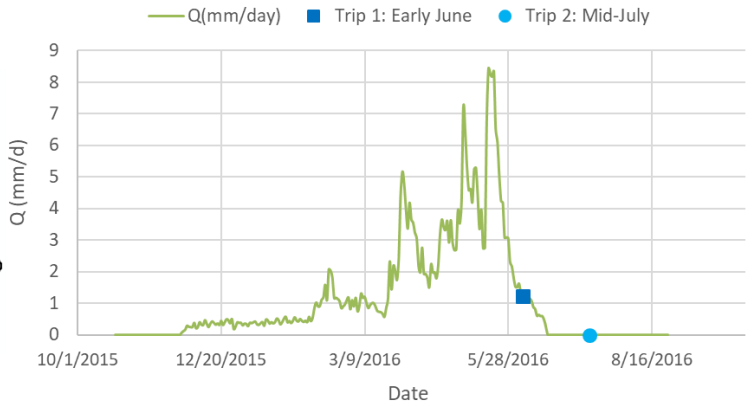
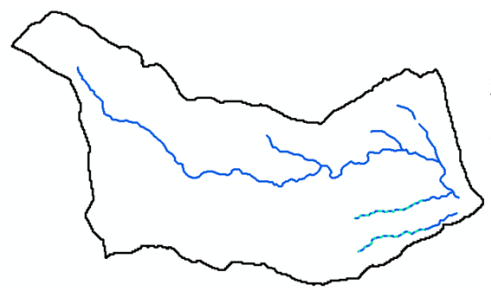
MU had a total stream length of 1,917 m with a disconnected length of 367 m and a stream density of $7.27 \times 10^{-4} \text{ m}^{-1}$ for trip 1 in mid-July (Table 3). Disconnected length is the length of the stream segment where surface water is unobserved, and the stream is flowing above and

below this segment (Figure 10). During trip 2 (late August), MU decreased to a stream density of $6.34 \times 10^{-4} \text{ m}^{-1}$; the flow initiation point moved further downstream, but the disconnected length remained the same. The discharge was small for both trip 1 and 2, 0.02 and 0.01 mm/d respectively. Even though the average discharge for MU was equal to MB, it did not flow year-round, but instead had 236 detected days of streamflow and discharge ranging from 0 to 3.16 mm/d.

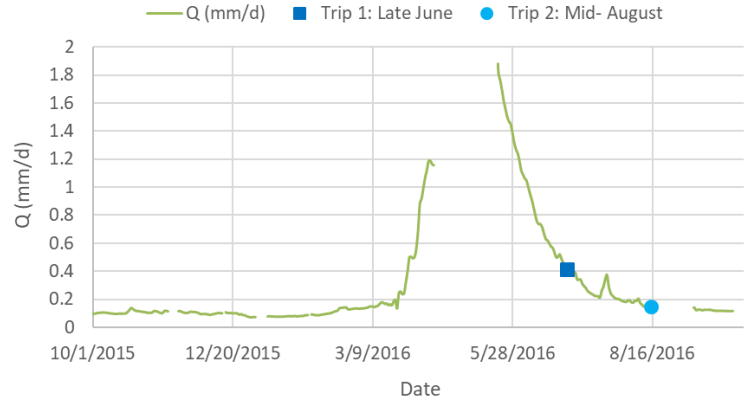
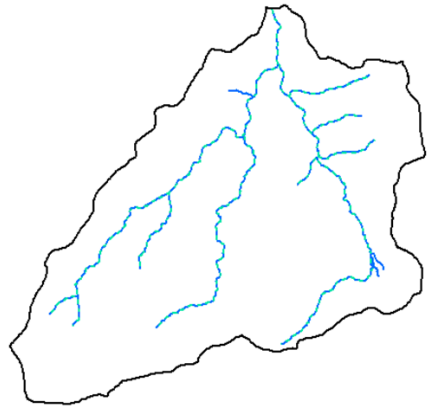
U had a stream length of 874 m and stream density of $5.09 \times 10^{-4} \text{ m}^{-1}$ for the first trip (mid-July) when snow cover obscured much of the channel network in the higher elevations (Figure 10). During the second trip (mid-August), two channel heads dried up, but four were gained upstream, resulting in stream length increasing to 1268m and stream density increasing to $7.38 \times 10^{-4} \text{ m}^{-1}$. Stream flow was disconnected along two channel segments with a total disconnected length of 166 m during the second trip. U flowed year-round with an average discharge of 2.64 mm/d. U had the largest discharge relative to other sites with a discharge of 6.88 mm/d for the first trip and 3.86 mm/d during the second trip. Streamflow at U was year-round with a mean discharge of 2.64 mm/d and a discharge range of 0.23 to 18.52 mm/d. The first survey of U is an incomplete representation of the channel network because the uplands were covered in snow.

L (Mill Creek)

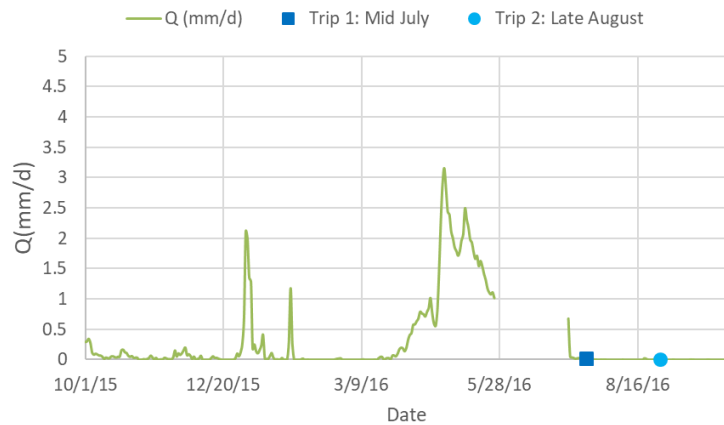
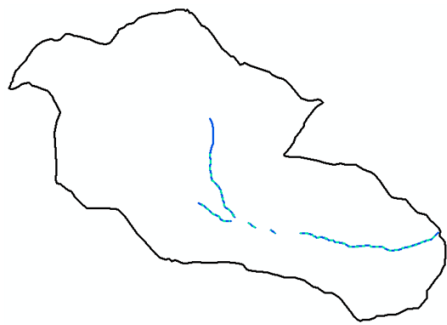
- Stream Trip 1
- - - Stream Trip 2



MB (Skin Gulch)



MU (Gordon Gulch)



U (Andrews Creek)

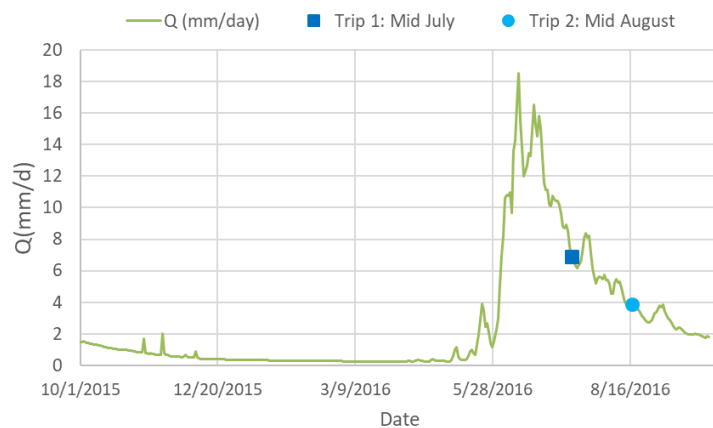
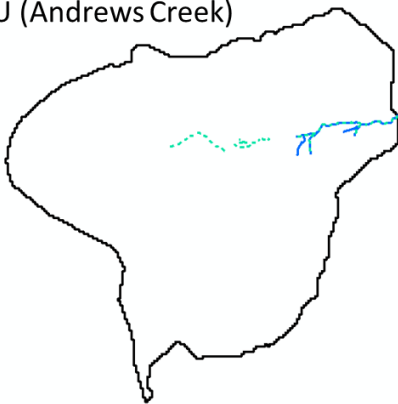


Figure 10. Field mapped stream networks from trip 1 and trip 2 (left) and hydrographs for WY2016 indicating when trip 1 and trip 2 were conducted (right). MU (Gordon) and MB (Skin Gulch) both have missing discharge data for part of the water year.

4.2. Topographic thresholds for deriving channel networks

Thresholds for TWI and $\ln(a)$ were the values that produced the closest (within 5%) channel lengths to the observed active stream lengths. Figure 11 shows stream lengths and stream densities and their respective TWI and $\ln(a)$ values for each study catchment. Channel length and stream density both decreased with increasing thresholds for stream initiation.

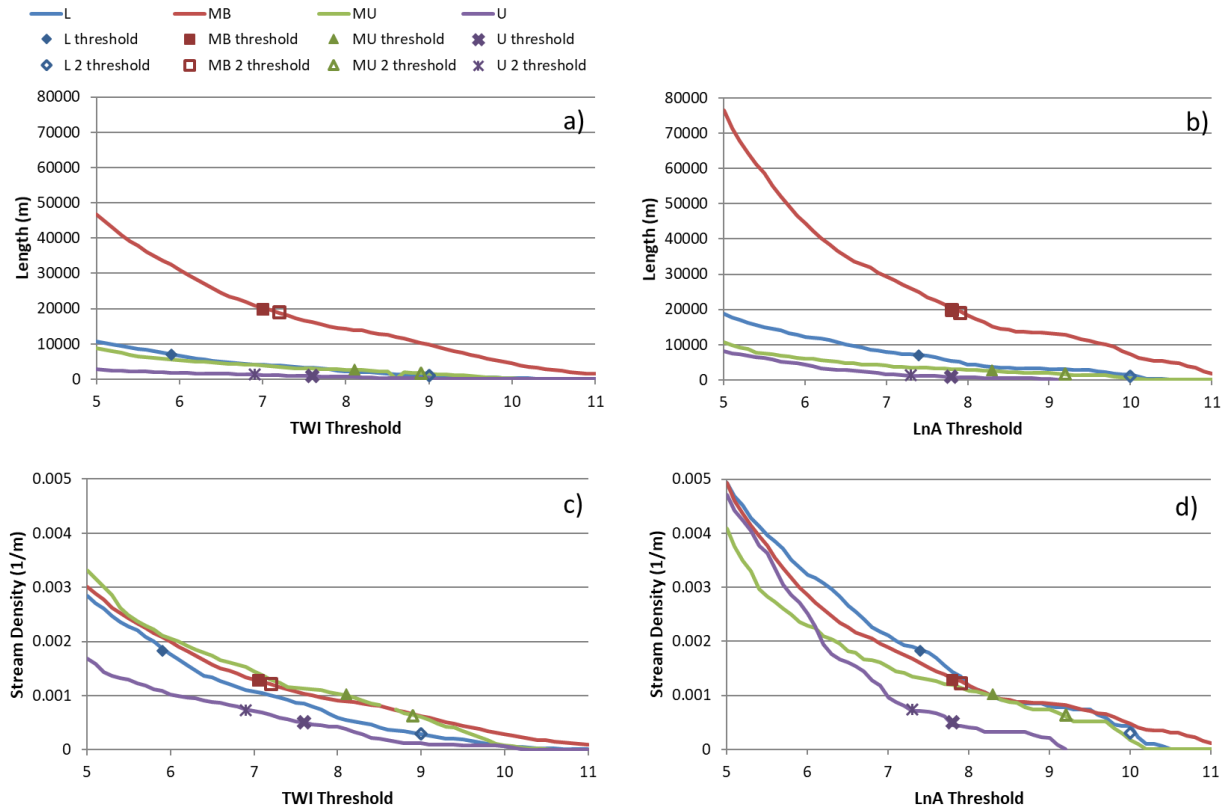


Figure 11. Changes in channel length and stream density (lines) for varying values of 10 m $\ln(a)$ and TWI thresholds for each watershed. Symbols indicate the lengths and stream densities for the field-mapped stream networks for trip 1 and 2.

Each watershed has a different relationship between the stream length or stream density and TWI and $\ln(a)$ threshold values (Figure 11). Because the catchments have different sizes and therefore different channel network lengths, comparison of these watersheds will focus on stream density. L, MB, and MU have similar patterns of decreases in stream density with threshold values, whereas U has lower stream densities for the same threshold values.

Threshold values varied across sites, DEMs, and trips as seen in Table 4. Using 10 m DEM resolution, L for trip 1 in early June had the smallest $\ln(a)$ threshold of 7.4 (163,598 m²), and MU for trip 1 (mid-July) had the greatest $\ln(a)$ threshold of 8.9 (183,300 m²). MB and U both

had $\ln(a)$ thresholds of 7.8, which is equal to an upslope accumulation area of 244,060 m². For Trip 2 (Mid July – August), the thresholds changed for every site, increasing at all sites except for U because all the channel networks changed length and stream density. L’s active channel network shrunk significantly and therefore had the greatest $\ln(a)$ threshold of 10, which is 2,202,600 m². MB’s threshold only decreased by 0.1 for both 10 m and 1 m, resulting in a decrease of about 25,640 m² for 10 m and 28,750 m² for 1 m. MU’s threshold increased to 9.2 (989,700 m²), and U’s decreased to 7.3 (148,000 m²).

Table 4. Threshold values of A, $\ln(a)$, and TWI for Trips 1 and 2 with 10 m and 1 m DEMs. A is the upslope accumulation area (m²) and $\ln(a)$ is the natural log of ‘a’ so that flow accumulation can be compared to TWI. TWI is the topographic wetness index, which is the natural log of upslope accumulation area over cell length divided by the natural log of slope (Equation 4).

Site	Trip 1						Trip 2					
	10 m Thresholds			1 m Thresholds			10 m Thresholds			1 m Thresholds		
	A	$\ln(a)$	TWI	A	$\ln(a)$	TWI	A	$\ln(a)$	TWI	A	$\ln(a)$	TWI
L	163598	7.4	5.9	183300	8.9	7.2	2202600	10	9	2467900	11.5	10.2
MB	244060	7.8	7	273450	9.3	7.8	269700	7.9	7.2	302200	9.4	7.9
MU	733194	8.9	8.7	890911	13.7	11.2	989700	9.2	9	984609	13.8	11.4
U	244060	7.8	7.6	540365	13.2	10.3	148000	7.3	6.9	488942	13.1	9.8

In all cases the all threshold values were higher for 1 m DEMs than for 10 m and also increased from trip 1 to trip 2, except for U which decreased due to increase in stream length. Relative patterns between sites, trips, and DEM resolutions for TWI thresholds were similar to those described for $\ln(a)$. The difference between TWI and $\ln(a)$ is the $\ln(\tan\beta)$ values, as shown in equation 7:

$$TWI = \ln\left(\frac{a}{\tan\beta}\right)$$

$$TWI = \ln(a) - \ln(\tan\beta)$$

$$\ln(a) - TWI = \ln(\tan\beta) \quad \text{(Equation 7)}$$

Where 'tanβ' is the slope and 'a' is the specific contributing area. Table 5 shows the ln(tanβ) values. Following equation 7, a greater difference between the ln(a) and TWI could indicate that slope has a greater role in the flow location (Table 5). Steeper slopes also have greater differences between ln(a) and TWI values. This creates an inverse relationship between TWI and slope where the larger the local slope the smaller the TWI value and therefore the smaller the TWI value will be from the ln(a) value.

Table 5. The difference of ln(a) and TWI from Trip 1 and Trip 2, where the values in the table represent ln(tanβ).

Ln(a) and TWI differences (ln(a) - TWI = ln(tanβ))				
Site	10 m		1 m	
	Trip 1	Trip 2	Trip 1	Trip2
L	1.5	1	1.7	1.3
MB	0.8	0.7	1.5	1.5
MU	0.2	0.3	2.5	2.4
U	0.2	0.4	3.5	3.7

All of the sites had greater ln(a) values than TWI threshold, but the differences varied from 0.1-1.35. At 10 m resolution, the effects of slope are greatest at L with ln(slope) of 1.5 and smallest for U and MU, where ln(slope) ranges from 0.2-0.4. At 1 m resolution, the pattern reverses, where effects of slope are greatest at U and lowest at L and MB. ln(slope) also has greater

values for 1 m compared to 10 m. $\ln(\text{slope})$ for 1 m ranges from 1.3-3.7 and an average of 2.26.

Trip 1 and Trip 2 have similar values only varying between 0 and 0.4 for 1 m DEMs.

4.3. Accuracy of derived channel networks

The derived channel networks and the channel networks from NHD (NHD High Resolution) were compared to the observed stream networks using the metrics described in section 3.2.2.

Figures 12 and 13 compare the spatial extent of the derived channel networks and NHD with the observed channel networks for trip 1 and trip 2.

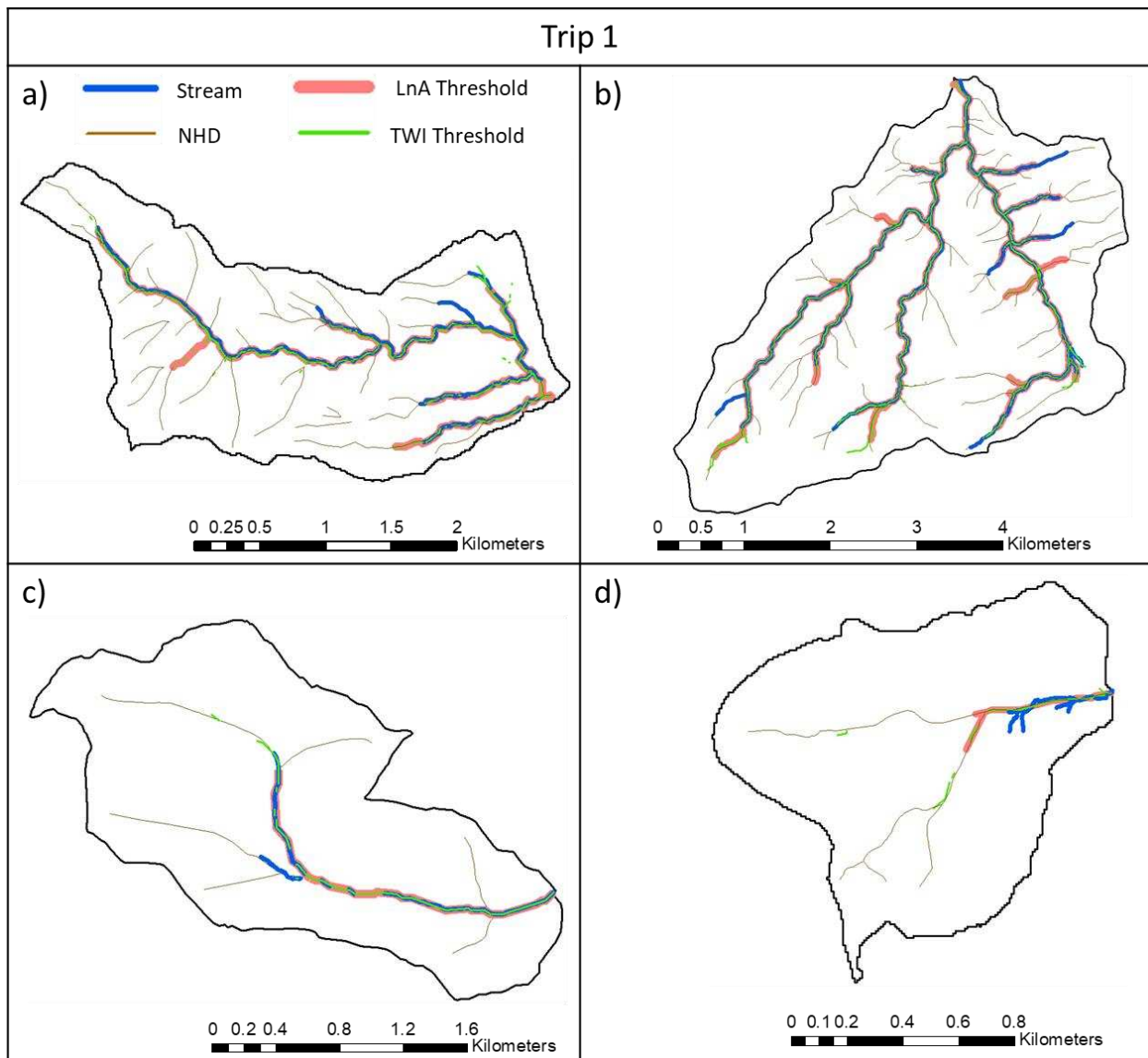


Figure 12. First Trip observed stream network (blue) compared with the first trip flow 10 m accumulation threshold (pink), 10 m TWI threshold (green), and NHD High Resolution network (brown). a) L with a $\ln(a)$ threshold of 7.4 and TWI threshold of 5.9, b) MB with a $\ln(a)$ threshold of 7.8 and TWI threshold of 7, c) MU with a $\ln(a)$ threshold of 8.3 and TWI threshold of 8.1, d) U with a $\ln(a)$ threshold of 7.8 and TWI threshold of 7.6. Note: stream width is not to scale, and each watershed is at a different scale.

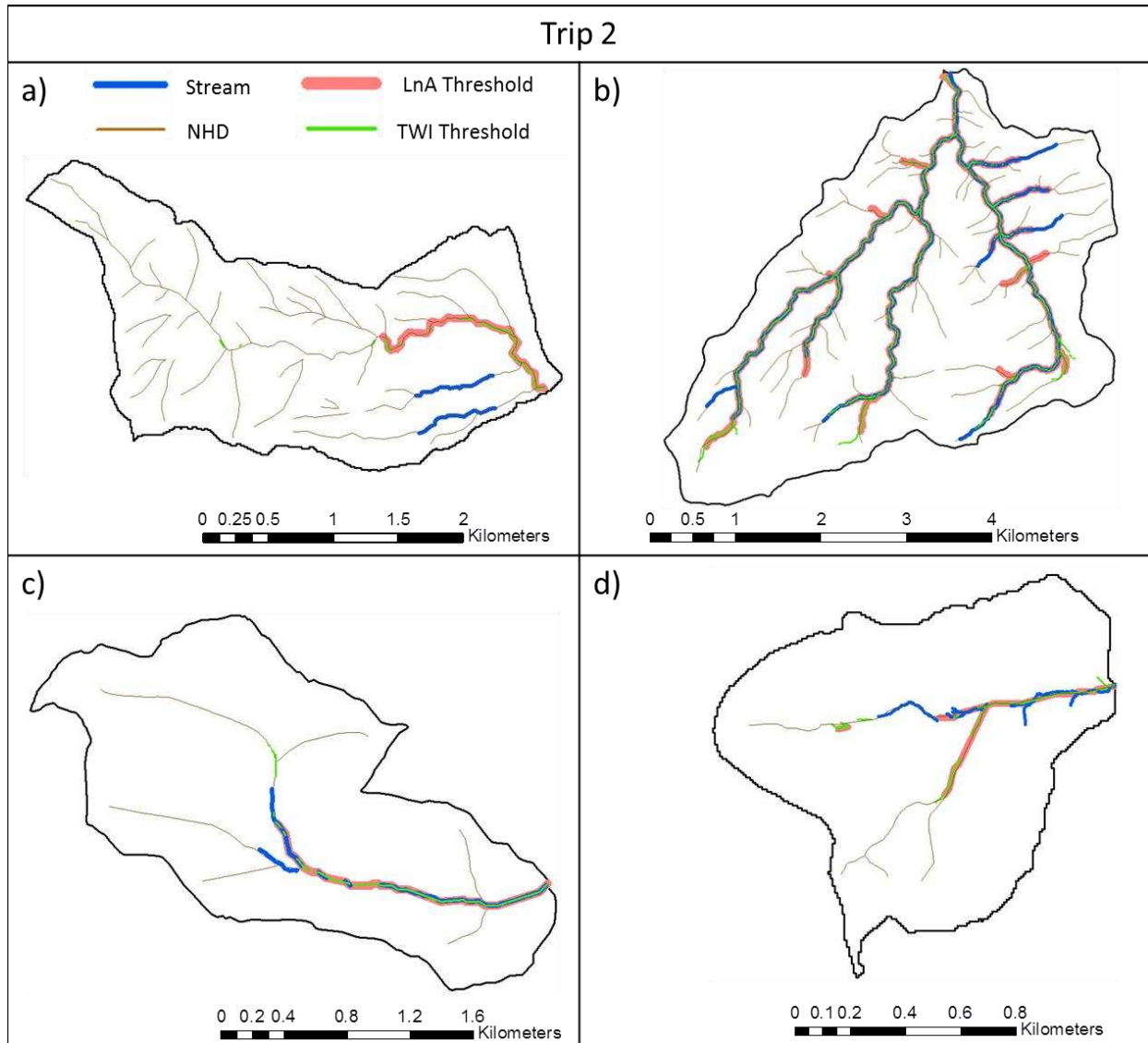


Figure 13. Second Trip stream network (blue) compared with the second trip flow accumulation threshold (pink), 10 m TWI threshold (green), and NHD High Resolution network (brown). a) L with a $\ln(a)$ threshold of 10 and TWI threshold of 9, b) MB with a $\ln(a)$ threshold of 7.9 and TWI threshold of 7.2, c) MU with a $\ln(a)$ threshold of 9.2 and TWI threshold of 8.9, d) U with a $\ln(a)$ threshold of 7.3 and TWI threshold of 6.9. Note: stream width is not to scale.

Visually NHD had the least accuracy of predicting the actual stream channel network; it had the most feathering and excessive number of tributaries that are counted as FP. For example, L had 30 extra tributaries, MB had 46, and MU had 4, while U tributaries were actually underrepresented. These extra tributaries produced a high percent of false positive errors, 63 -

94% (Table 6); however, NHD had no false negatives (FN), except at U (26-35%). Overall, NHD had the lowest accuracy at U (25%) and highest accuracy at MB (43%) for trip 1. For trip 2, the lowest accuracy for NHD was at L (6%) and highest again at MB (41%).

For the lowest elevation site, L, the channel networks derived from topographic thresholds had a wide range of performances. For Trip 1, TWI produced 6 more small tributaries (FP) than were observed in field, and these derived extra tributaries were discontinuous (Figure 12). $\ln(a)$ in trip 1 only predicted 1 more tributary than observed (FP), but it was continuous. Both TWI and $\ln(a)$ did not map a small flowing tributary (FN) from the first trip. Even though the thresholds mapped extra tributaries, TWI and $\ln(a)$ had the greatest total accuracy of all watersheds in Trip 1, with accuracy ranging from 89-91% and lowest FP and FN % ranging between 9-11% (Table 6). In trip 2, TWI and $\ln(a)$ produced mapped stream locations that were far from the actual stream network because the thresholds predicted the main tributary as flowing, whereas only the south small tributaries were actually flowing (Figure 13). Both $\ln(a)$ and TWI were completely incorrect, giving 0% accuracy and FP of 100%. Overall the derived channel networks from TWI and $\ln(a)$ at 1 m and 10 m were similar for L.

Thresholds generally produced good representations of the MB channel network. MB had high accuracy thresholds for both Trip 1 and Trip 2 with a range of 84-90% (Table 6). Some minor discrepancies in the threshold predictions were that $\ln(a)$ and TWI predicted seven extra tributaries (FP) in MB that were not in the mapped stream network and created longer streams for three MB tributaries (FP) (Figure 12 and 13); even with these errors, overall FP was low with

13-14% for ln(a) in 10 m and 12-15% in 1 m resolution grids. Because MB did not change much in length (less than 5%) between trips, the derived networks were similar visually between trip 1 and 2. In trip 2, some small tributaries had dried up, but the thresholds still mapped them as flowing, leading to more FN errors. For Trip 2, 1 m performed slightly better in FN, with 10% lower FN than 10 m for both ln(a) and TWI, whereas 10 m performed better for FP, with 6% lower FP for TWI.

Table 6. Accuracy assessment of the derived channels compared to observed channels. FP is the % false positive and FN is % false negative. % Accuracy is the total % of the derived network length that is correct.

Trip #	Site	10 m						1 m						NHD		
		ln(a)			TWI			ln(a)			TWI			FP	FN	%
		FP %	FN %	% Accuracy	FP %	FN %	% Accuracy	FP %	FN %	% Accuracy	FP %	FN %	% Accuracy	%	%	Accuracy
Trip 1	L	10	10	90	11	11	89	9	10	91	11	10	89	63	0	37
	MB	14	13	86	16	15	84	12	14	88	14	17	88	57	1	43
	MU	24	21	78	16	22	84	24	20	76	23	20	77	67	0	33
	U	49	19	21	54	43	46	26	55	74	44	47	56	75	26	25
Trip 2	L	100	0	0	100	0	0	100	0	0	100	0	0	94	0	6
	MB	13	27	87	14	33	90	15	18	85	20	22	80	59	0	41
	MU	22	25	78	35	30	83	27	20	73	24	21	76	71	0	29
	U	72	48	28	70	46	30	42	42	58	27	29	73	64	35	36
Average		38	20	59	39	25	63	32	22	68	33	21	67	69	8	31

For MU, topographic indices performed differently especially using different resolution DEMs. The overall accuracy was good (73 – 87%), and both ln(a) and TWI predicted the headwaters for the main stream to be further upstream than observed in the field. ln(a) had a total accuracy of 78-87% for 10 m and 76-73% for 1 m (Table 6), whereas TWI had a total accuracy of 84-83% for 10 m and 77-76% for 1 m (Table 6). Neither of the thresholds captured the spatially

discontinuous stream flow found at MU (Figure 13), which increases the FP. FP and FN for MU were relatively higher than at L and MB, ranging between 16 -35%. MU's thresholds for trip 2 did not predict the southwestern 1st order tributary to be flowing.

U had a poor performance from all the thresholds for both trips. For 10 m, U had 21 - 28% accuracy for ln(a) and 30 - 46% accuracy for TWI (Table 6). For 1 m, U's accuracy increased for ln(a) and TWI, 58 – 74% and 56 – 73% respectively (Table 6). U was the only watershed for which 1 m performed consistently better than 10 m. The number of active channel tributaries at U was greater than predicted by TWI and ln(a) resulting in a high FN% for U (Figure 12 and 13). These tributaries formed from saturation excess overland flow and were not captured well by the topographic thresholds, leading to FN errors. Also the derived networks falsely showed the stream to be flowing further upstream (FP) from the channel heads in the area that had a rock glacier. FP and FN were greatest for U with values between 27 – 72% when comparing to other sites. Many errors contributed to the high FP and FN including both thresholds did not capture the spatially discontinuous flow along the main channel, they missed a significant segment of flow furthest upstream and three small tributaries, and they produced a large 1st order tributary that was not observed in field.

Comparing the average FP, FN, and % accuracy of all sites, ln(a) and TWI performed similarly with equal to or less than 5% differences (Table 6). Comparing 1 m and 10 m, both ln(a) and TWI had the best average accuracy for 1 m, which increased the average accuracy for ln(a) by 9% and for TWI by 4%. NHD performed the worst overall, with only an average of 31% accuracy,

and it greatly overestimated the number of tributaries and the length. By site, the greatest accuracy in trip 1 was for L (91% for ln(a) 1 m), followed by MB (88% for ln(a) and TWI 1 m), MU (84% for TWI 10 m), and U (74% for ln(a) 1 m). In trip 2, greatest accuracy was for MB (90% for TWI 10 m), followed by MU (83% for TWI 10 m) and U (73% for TWI 1 m).

Table 7. Quantitative results showing the number of stream tributaries during each trip (#) for observed and derived channel (ln(a) and TWI) networks. ‘#OT’ is the number of observed tributaries that represent the field stream locations. ‘#DT’ is the number of derived tributaries. ‘# correct CH’ is the number of correctly identified channel head locations (channel initiation locations).

DEM	Site	Trip 1					Trip 2					NHD			
		Field		ln(a)		TWI		Field		ln(a)		TWI		#DT	# correct CH
		#OT	# DT	# correct CH	#DT	# correct CH	#OT	#DT	# correct CH	#DT	# correct CH				
10 m	L	6	7	2	11	3	2	1	0	1	0	36	0		
	MB	12	17	2	21	2	9	16	1	18	0	58	1		
	MU	2	2	1	2	0	2	1	0	1	0	6	0		
	U	5	2	0	3	0	7	3	0	3	0	4	0		
1 m	L	6	6	1	8	2	2	1	0	1	0	36	0		
	MB	12	15	2	22	1	9	14	1	20	0	58	1		
	MU	2	1	0	2	0	2	1	0	2	0	6	0		
	U	5	1	0	4	0	7	2	0	5	0	4	0		
Total		50	51	8	73	8	40	39	2	51	0	208	2		

Even though the total accuracy of the stream networks produced by the topographic indices was good in most cases, channel head locations were not represented well by thresholds, as they were either too far upstream or downstream (Table 7). Only 16 out of 124 channel initiation points created by thresholds for 10 and 1 m were correct for trip 1, and only 2 out of 90 channel initiation points produced by thresholds for trip 2 were correct. TWI overall

produced more channel heads, but both $\ln(a)$ and TWI had about the same number of correctly identified channel heads (or tributaries). NHD produced six times more tributaries than were observed for L and MB and three times more than were observed for MU.

4.4. Catchment comparisons

Comparing the four study watersheds, the highest elevation site (U) had the largest discharge during both trip 1 and 2. Discharge generally increased with catchment elevation, snow persistence, and precipitation, with the exception of MU, which had the lowest discharge (Figure 14c, 15c). In contrast, stream density was lowest at the highest elevation site (U) and highest at the low elevation site (L) during trip 1 (Figure 14a). Excluding the burned site, days of flow also increased with elevation and precipitation but had a weak increasing trend with stream density (Figure 14b, 15b). Stream density and annual precipitation are not clearly correlated (Figure 15a), whereas stream density has a strong negative correlation with elevation for trip 1 and no correlation for trip 2 because L's channel network shrinks so much (Figure 14a).

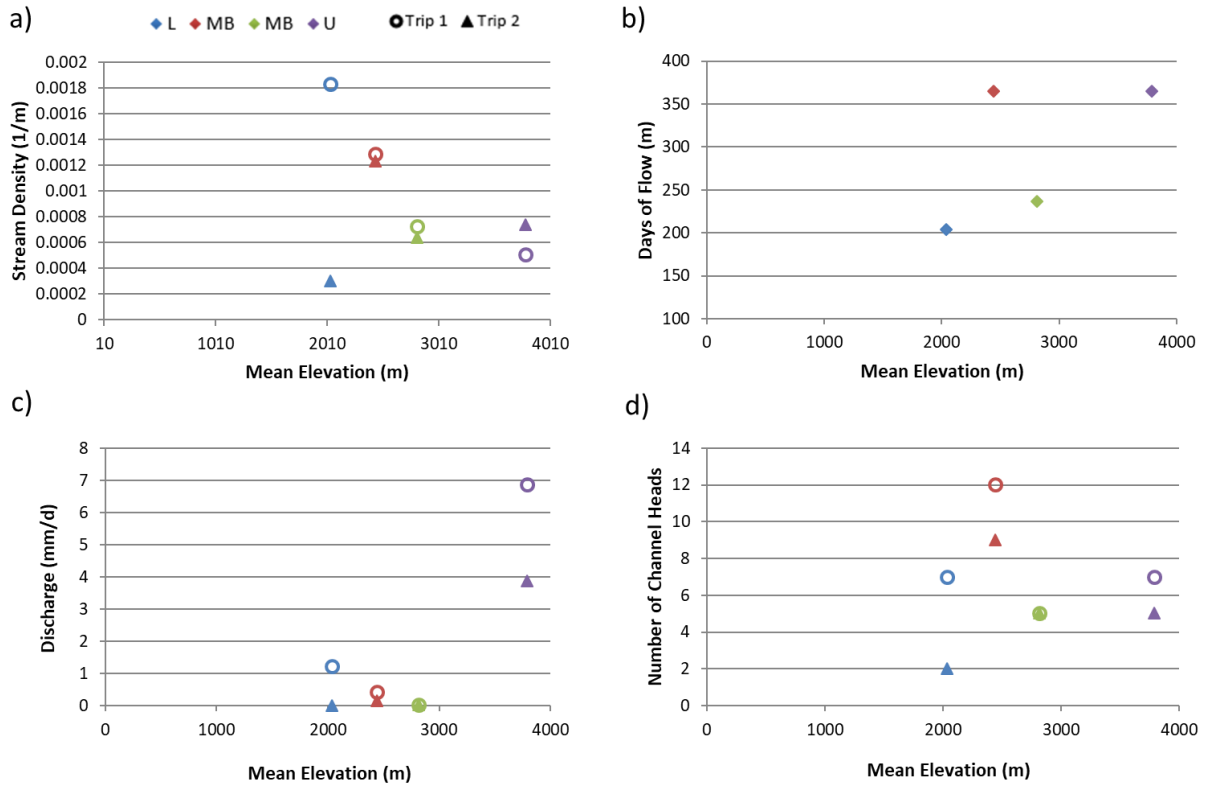


Figure 14. Mean elevation relationships with stream density (a), days of flow (b), discharge (c), and number of channel heads (d).

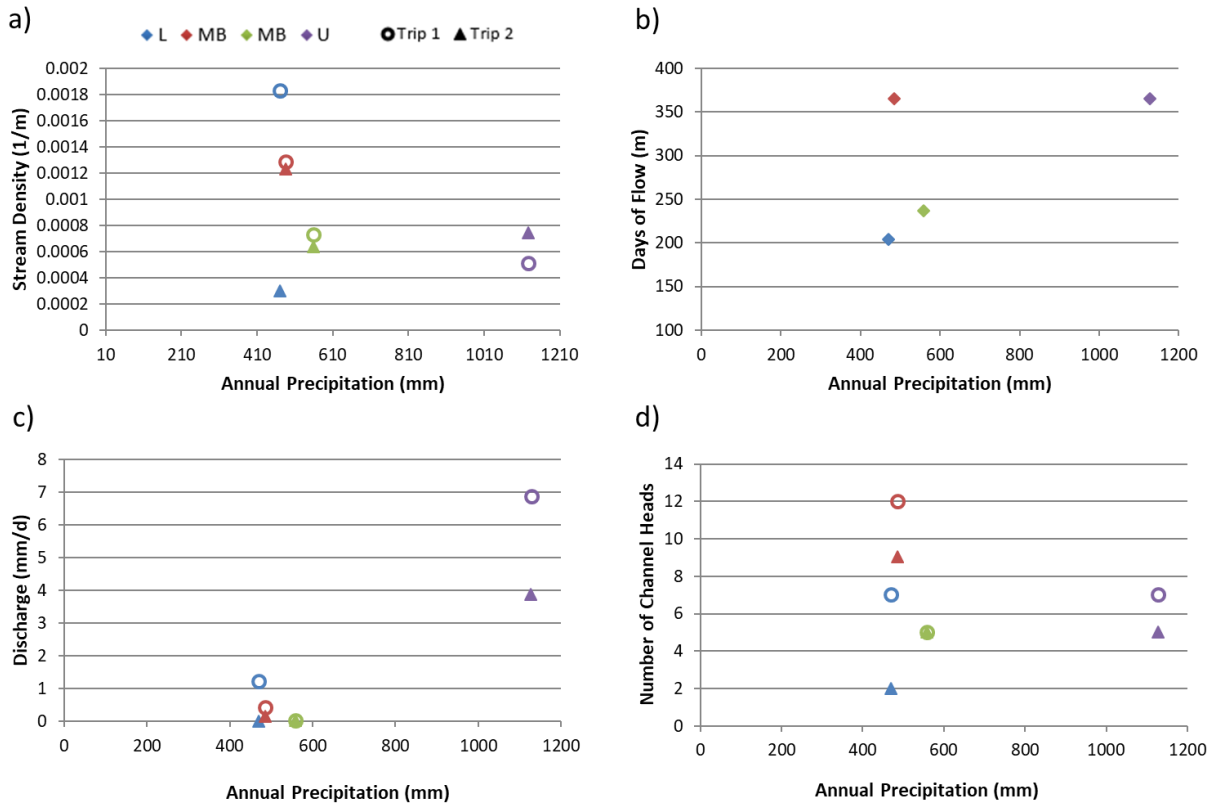


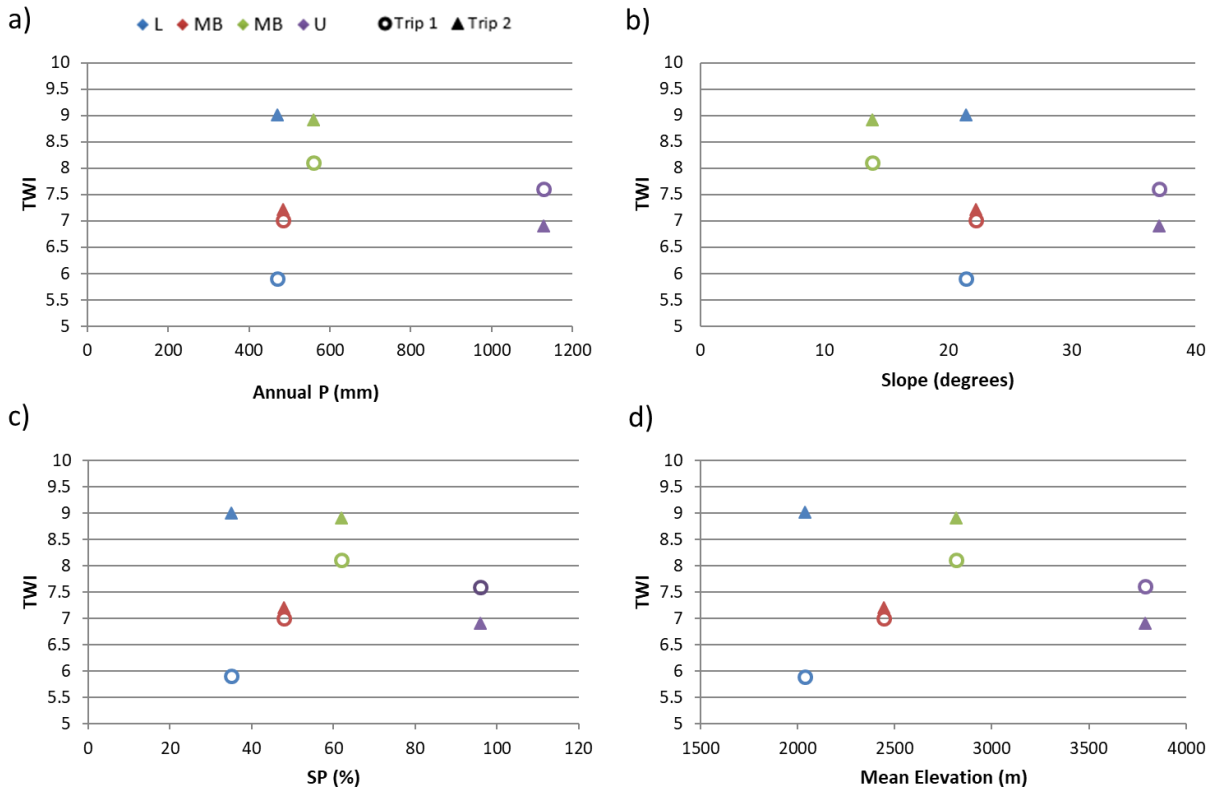
Figure 15. Annual 2016 precipitation relationships with a) stream density, b) days of flow, c) discharge, and d) number of channel heads.

To examine what causes variability in TWI and $\ln(a)$ thresholds, I compared precipitation, slope, SP (snow persistence), elevation, drainage area, discharge, stream density, and number of channel heads to the TWI and $\ln(a)$ threshold values across sites (Figure 16). $\ln(a)$ and TWI had similar relationships to these variables, so only TWI is shown here. Mean annual precipitation and mean slope are not clearly related to TWI thresholds (Figure 16a,b), whereas thresholds generally increase with increasing SP and elevation for trip 1 except at the highest elevation site, U, where the values decrease (Figure 16c). For trip 2, this trend is not repeated because L's threshold greatly increases. The $\ln(a)$ and TWI thresholds have the greatest range in values for the lowest elevation site, L, which was mostly dry during trip 2. Lower TWI thresholds generally correlate with lower stream density and number of channel heads (Figure 16g,h), whereas,

drainage area, and discharge have little apparent connection to TWI thresholds (Figure 16e,f).

TWI thresholds also increase with the sand % and saturated hydraulic conductivity ($\mu\text{m/s}$)

values from the USDA web soil survey (Figure 16i,j).



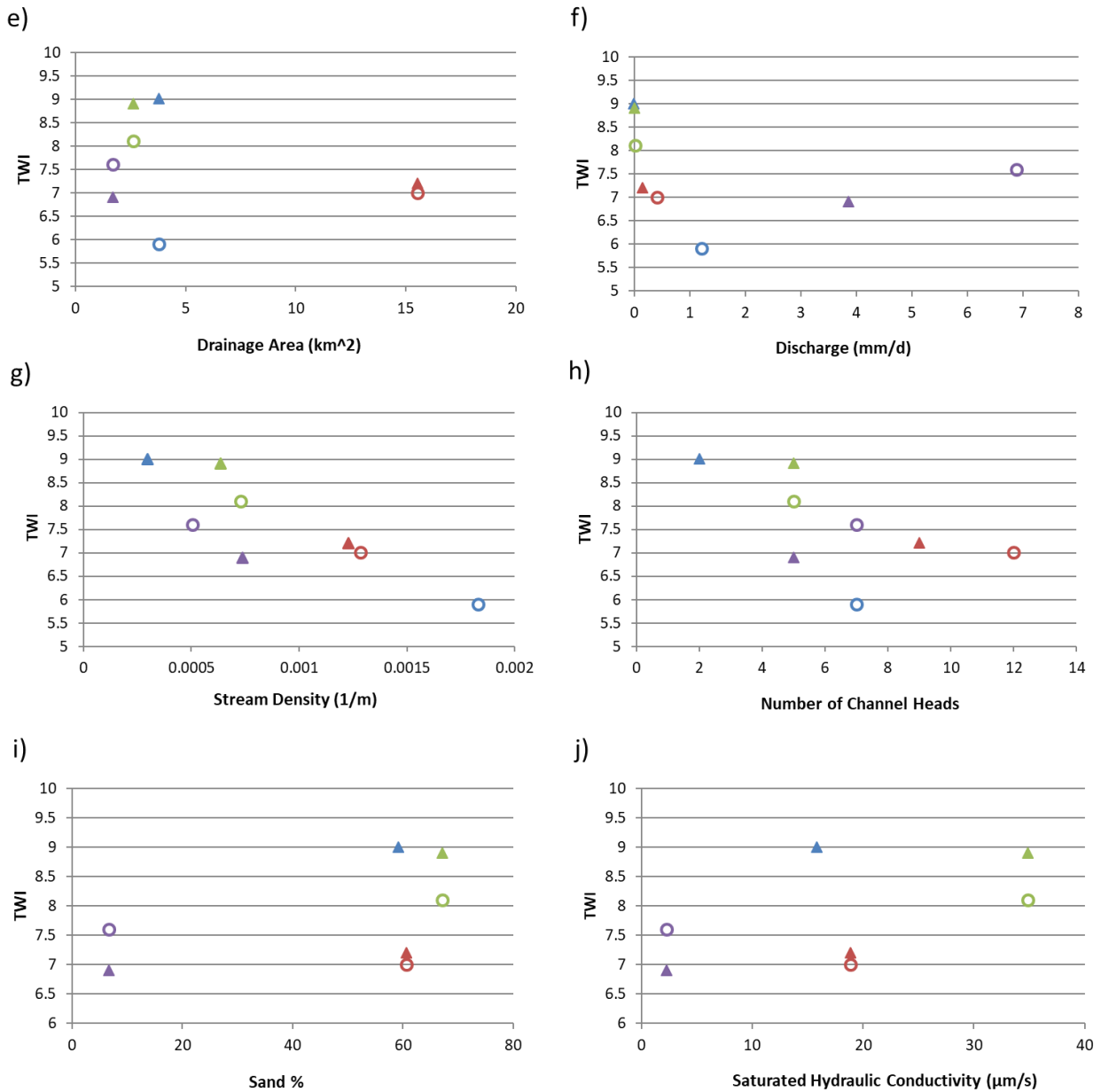


Figure 16. Variation in TWI thresholds for each watershed and trip with climate factors and watershed characteristics: (a) 2016 annual precipitation, (b) mean slope, (c) mean annual 2016 Jan-Jun snow persistence (SP), (d) mean elevation, (e) drainage area, (f) discharge, (g) stream density, (h) number of channel heads, (i) sand %, and (j) saturated hydraulic conductivity.

Differences in the correlations of TWI thresholds with elevation, SP, and precipitation can be explained by how these variables relate to one another (Figure 17). Elevation and mean annual precipitation have a nonlinear relationship, where precipitation does not change much

between lower and mid elevation sites but increases substantially at the highest site (Figure 17a). SP in contrast increases linearly with elevation and nonlinearly with precipitation (Figure 17b, c).

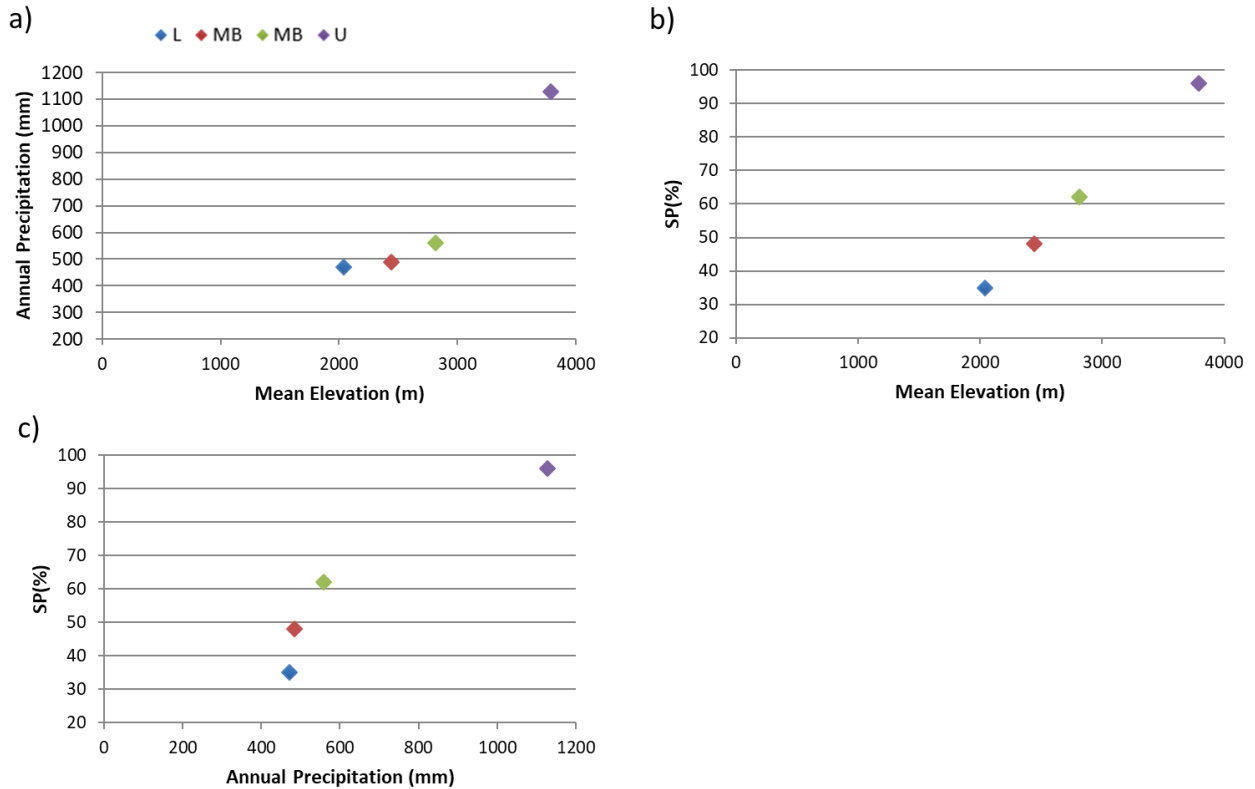


Figure 17. Comparison of elevation and climate variables and their effect on stream density. a) 2016 annual precipitation vs mean elevation, b) 2016 SP vs mean elevation, c) 2016 SP vs annual precipitation.

4.5. Physical catchment characteristics affecting stream networks

The differences between topographically derived channel networks and field maps may relate to physical factors such as geology, soil, vegetation, and aspect. I examined maps of each of these factors to evaluate qualitatively their influences on the stream networks.

4.5.1. Geology

L's channel head starts along a fault. An NDVI image of L created from a Landsat-8 image courtesy of the U.S. Geological Survey shows that even when the majority of watershed is dry during July, the headwater along the fault retains high NDVI values (Figure 18a). Also, L's stream flows mostly along the quartzofeldspathic mica schist (Figure 18). During the second trip, streams only flowed on trondhjemite, and flow was no longer evident on the surface where the channel is overlying the conglomerate, indicating that surface water most likely infiltrated in this area.

The two main 2nd order streams and one 1st order stream of MB flow along the shear zones in MB (Figure 18b). The headwaters of the western tributary start in amphibolite or granodiorite, and the stream mostly flows along amphibolite and schists while circumventing pegmatite. The MU stream network heads in alluvium then passes through the contact between foliated monzonite and unfoliated monzonite (Figure 18c). Areas of disconnected flow are at the contact between unfoliated monzonite and granodiorite.

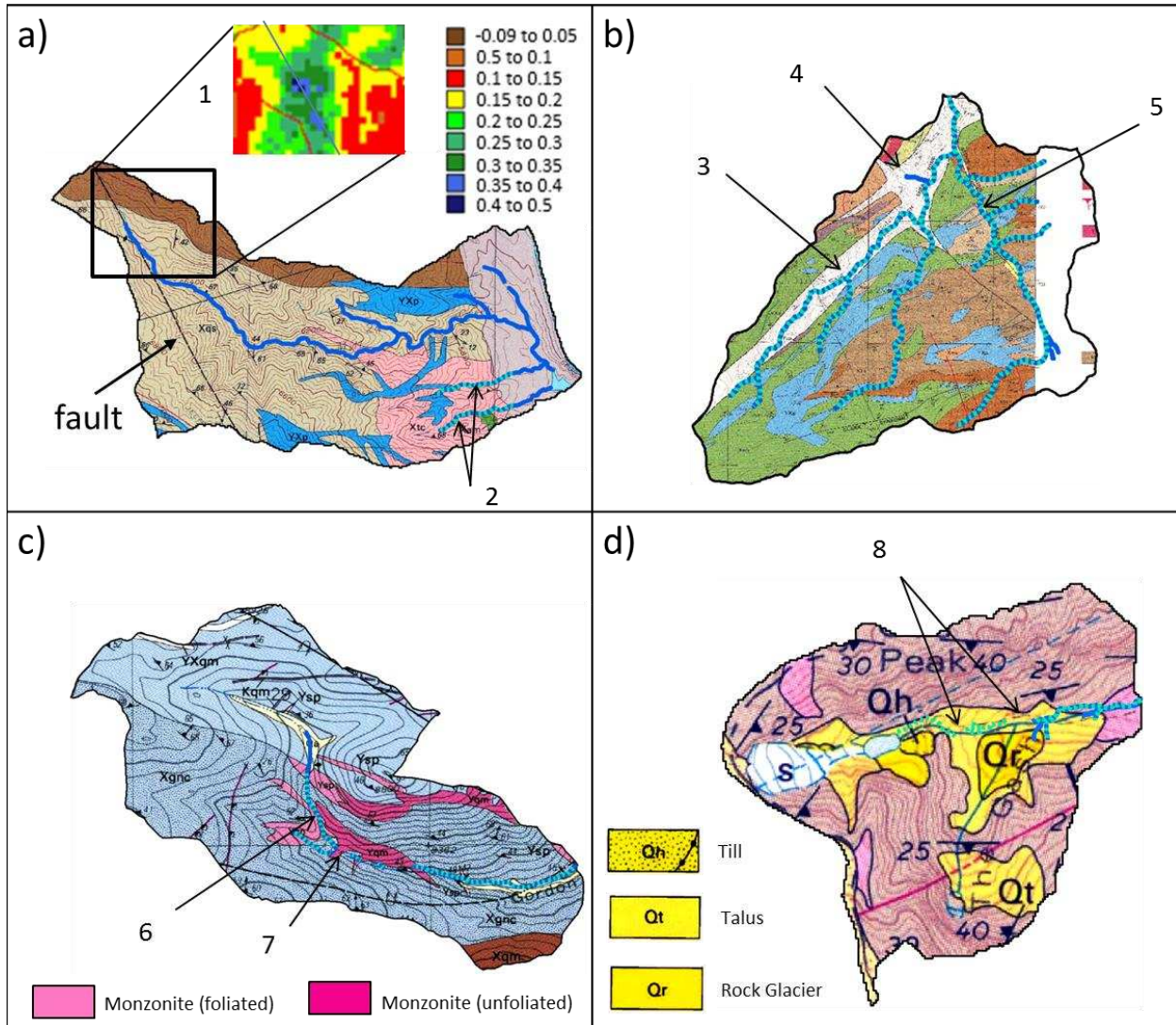


Figure 18. Geologic maps of all sites highlighting connections between geology and stream locations. (a) L, highlighting the high NDVI values for the headwaters (1) and streams that were flowing on trondhjemite during the second survey (2), (b) MB showing streams located on shear zones (3,4,5). (c) MU showing stream flowing along bedrock contact (6) and stream network disappearing over unfoliated monzonite (7), (d) U showing discontinuous streamflow on talus and rubble (8).

U's watershed is much different from the other sites. It is glaciated terrain covered with 30% talus and 53% bedrock (Clow et al., 2003), as the U-shaped valley was carved by a glacier leaving behind talus and till. This valley is where the stream flows, and this flow was spatially discontinuous along the talus and rubble; it flowed on the talus in some areas but then

disappeared in others (Figure 18d). The stream also flows around till and rock glacier and stays on the talus and then is spatially continuous in the lowlands where thin soil developed over the till.

4.5.2. Soils

Sandy loam makes up the majority of the soil types in the study sites. The upslope area of L is all sandy loam, and the stream flows mainly over sandy loam in the upper watershed. At lower elevations, the slope is flatter, and the soil type changes to loam. L had flow mainly over the loam the second trip, with no flow remaining in the area with sandy loam soils. The streams of MB mostly flow over loam, but all upslope and surrounding soil is sandy loam. Similarly, SSURGO survey data show loam along MU's stream, but all of the upslope area is sandy loam. U flows through talus and over rock outcrop and then sandy loam is downstream of the break in slope, where the meadow sits. The soils at MU and U are "somewhat excessively drained" while L and MB soils are well drained (Soil Survey Staff). U has the highest available water capacity average of 86.22 cm/cm, whereas the others have less than 0.13 cm/cm (Soil Survey Staff, 2016). MU has the greatest saturated hydraulic conductivity with 31.72 $\mu\text{m/s}$. MB, U and L have Ks as 20.15, 20.87, and 17.89 $\mu\text{m/s}$, respectively.

4.5.3. Vegetation and Aspect

Vegetation type was correlated with aspect, elevation, and slope, but the resolution of the National Land Cover map used in this study is most likely too coarse for interpreting vegetation effects on small headwater stream locations. The type of trees that dominate the watersheds

depended on the elevation. The dominant vegetation type in the lowest elevation watershed is ponderosa pine and mixed conifer in the uplands where slopes are steeper, and shrubs and grasses were in the lowlands where the slope is <10%. MU and MB both have ponderosa pine, lodgepole pine, and mixed conifers, however MB only has lodgepole pine at the headwaters whereas MU has more lodgepole pine throughout the catchment. Visual trends of aspect and vegetation were observed where ponderosa pine was found more commonly on south aspects and conifers were found more commonly on north aspects. Aspens were also more commonly found on north aspects at MU and MB and along the headwaters at MB. These aspect-dependent vegetation patterns had no evident effect on stream locations. U does not have much vegetation because it consists of bedrock and talus, but near the lowlands and gentle slope areas the watershed has alpine vegetation or spruce-fir forests. All of the watersheds have riparian vegetation in patches along the channel corridors, although these vegetation types did not always be represented in all of the land cover maps. Where riparian vegetation and soil developed along U's channel was where water exfiltrated to the surface. Some riparian vegetation was mapped further upstream on MU where no observed streamflow was evident during surveys.

5. DISCUSSION

Results suggest that topography, geology, and soils all affect flowing stream location and duration. These interact with climate, which affects how long the streams flow. Each of the study catchments tells a different story on the movement of water.

5.1. Lower (L)

L, the lowest elevation site, had the most frequent small pulses of discharge throughout the early water year especially during rising limb and peak flow, but then it quickly dried up giving a short falling limb (Figure 10). This is common at lower elevation sites along mountainous catchments due to the infrequent small snow events that melt quickly and provide a pulse of flow to the streams (Richer et al., 2013). L started flowing November 28, 2015 and stopped flowing June 28, 2016, but these discharge measurements were only on the main stem that dried up on this date, whereas other tributaries were still flowing. Geology evidently influenced the duration and location of streamflow during trip 2, when the discharge was low, as flow continued on the trondhjemite, which is a type of granite, and dried up over quartzofeldspathic mica schist (Figure 18a). These two tributaries stopped flowing once they intersected the conglomerate downstream of the trondhjemite. This suggests that flow dissipates as it hits the more porous medium, the conglomerate/sandstone, which is a sedimentary rock with a mix of grain sizes including fine sand and gravel or larger particles. Sandstone is highly permeable/erodible and has high hydraulic conductivities (Heath, 1983) (Figure 19). This suggests that lithology can affect hydrologic connectivity and water storage capacity, which

then influences the duration of surface flow. Flow over loam was spatially discontinuous in one location but had longer duration in L, which suggests that the lower hydraulic conductivity loam stored water longer than the sandy loam elsewhere in the catchment. These results are in agreement with Güntner et al. (2004) among many others who have found that saturated areas were twice more likely in areas with poorly conductive soils than in those with higher conductivities.

Other studies have found that lithologies with high hydraulic conductivities such as sandstone are more hydrologically connected (Jensco et al., 2009; Payn et al., 2012) and exhibit a positive correlation with mean response time (Nippgen et al., 2011). This could explain why, even though the stream locations were usually over porous/permeable/erodible lithologies, the duration of the stream flow was shorter for these rock types compared to the more impermeable bedrock lithologies such as granite, pegmatite, and trondhjemite. Because flow remained on trondhjemite, it suggests that this rock type or the soil derived from it can hold water for longer and supply subsurface flow to the stream. This finding agrees with Onda et al., (2006) who found that in steep mountains subsurface stormflow was evident in soil mantle with granite as the parent bedrock.

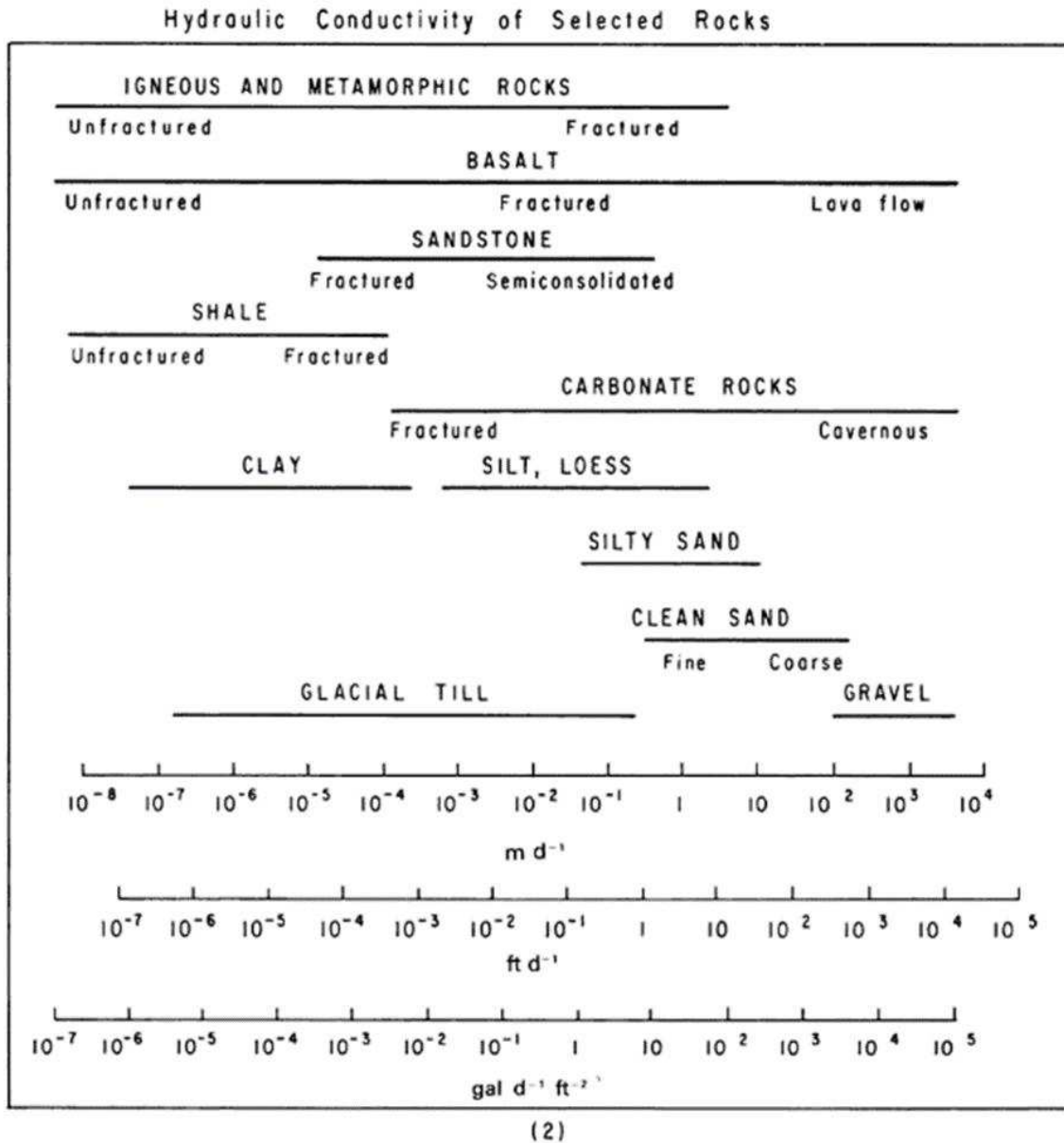


Figure 19. Hydraulic conductivities, K, for different rock types (Heath, 1983).

L's headwaters also followed a fault for 400 m, and an NDVI image (Figure 18a(1)) indicated that where the headwaters and fault intersected, the stream was wet and plants were green (NDVI = 0.3-0.41) even when the rest of the catchment was dry (NDVI = 0.15 -0.05) during July. This suggests that this fault was acting as a conduit for groundwater to the subsurface, as was observed in other studies (Uhlenbrook et al., 2002).



Figure 20. MB's (Skin Gulch) channel bed that is wide, armored with coarse sediments, and includes segments of exposed bedrock.

5.2. Middle burned (MB)

The burned site (MB) had a continuous supply of flow all year long, with peak flow during spring snowmelt. The continuous flow may be due to the effects of the fire, as residents of the area have noted that it used to dry up before the fire (Kampf et al., 2016). Even though discharge magnitude decreased from the first trip to the second trip, the streamflow locations only decreased by 5% of the stream length from trip 1 to 2. This could indicate that the stream is supplied by a continuing groundwater source. Also, because this site was burned and then impacted by a large flood (Brogan et al., 2017), the hillslopes and channel have been heavily eroded, resulting in a wide channel armored with boulders. Little riparian zone remains, which

decreases the likelihood that the channel could lose surface flow into the riparian zone. In addition, vegetation along hillslope is sparse leading to a decrease in transpiration losses. The channel flows along amphibolite and mica schist while avoiding impermeable pegmatite, and the majority of Skin Gulch's stream network follows shear zones and faults (Figure 18 b(3,4,5)). This drainage pattern where the streams follow shear zones and faults is considered a trellis drainage; other surrounding watersheds had similar trellis drainages (Figure 21)

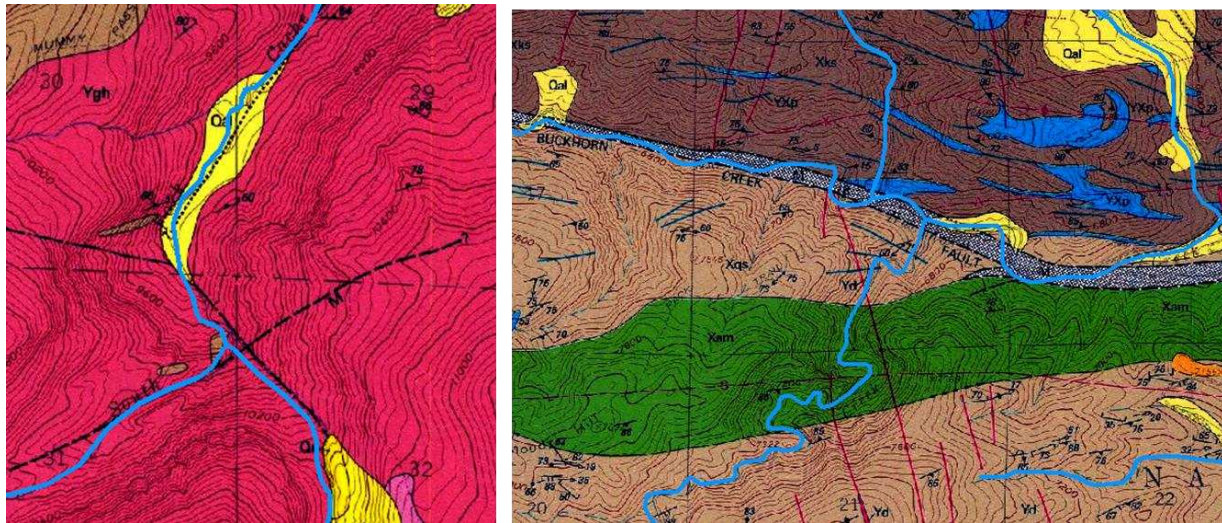


Figure 21. Example of other streams near MB (Skin Gulch) that had streams that followed shear zones and faults.

Faults/shear zones could be weak points in the bedrock that have lower resistance and therefore be areas more likely to become incised and concentrate streamflow. These observations agree with Güntner et al. (2004) who found that areas along faults were more likely to be saturated than areas more distant from faults. Also, mica schists and amphibolite (metamorphic rocks) can have high hydraulic conductivities like sandstone if they are fractured, allowing greater erodibility and creating preferred paths for streams.

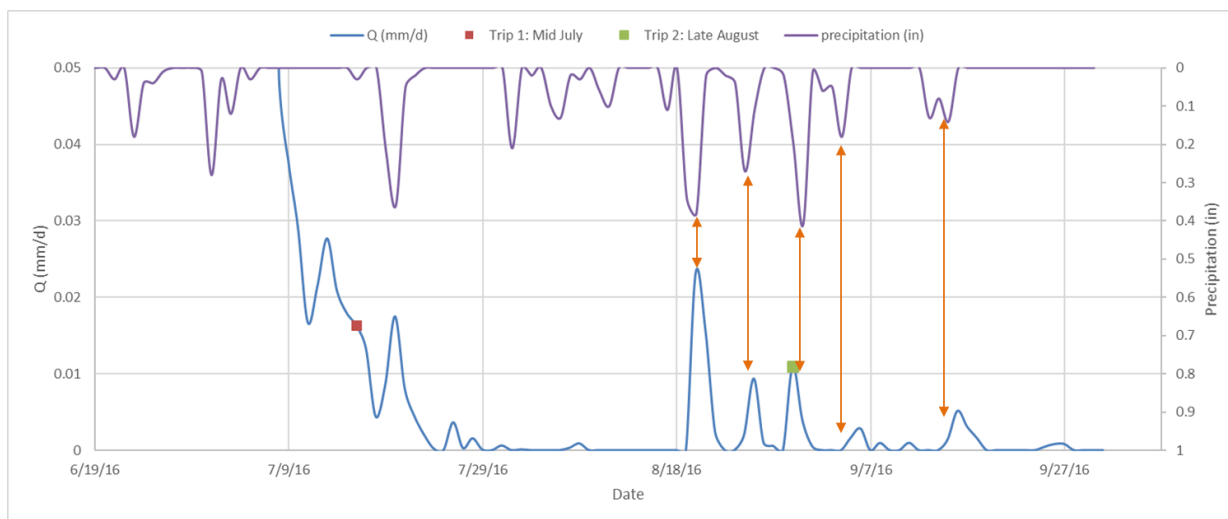


Figure 22. Summer rain events led to flow in Gordon Creek (MU) during August and September. The orange arrows are pointing the rain events and the resulting streamflow.

5.3. Middle unburned (MU)

The MU site had 236 days of streamflow (with 42 days of missing data) throughout the 2016 water year. It dried up a couple times during the winter and in the late summer. It is possible during the winter that the stream was frozen, interfering with the stream stage measurement. During the dry periods in late summer the stream did start flowing again in response to rain (Figure 21), which indicates that either overland flow occurred, or the catchment was wet enough that rain storms reactivated subsurface flow paths, which agrees with Heckman (2012) who found that the stream chemistry responded to rain. Discharge decreased from trip 1 to trip 2 and resulted in a 13% decrease in stream length on the north tributary. Toward the headwaters Gordon Creek flows between the bedding contacts of unfoliated monzonite and foliated monzonite (Figure 18c(6)). Bedding contacts could also be considered a path of least resistance for water to preferentially flow along, creating fracture flow (Payn et al., 2012). At MU the disappearance of flow along the channel was more difficult to interpret. Segments of

the stream did not have surface flow over the unfoliated monzonite, and surface flow then reappeared along the foliated monzonite (Figure 18c(6)). Because unfoliated monzonite (granite-like) is theoretically more impermeable, possibly the water does not exfiltrate there and instead flow reappears downstream where the more permeable gneiss is located. The gneiss is most likely more permeable due to more fractures and aligned minerals from deformation, allowing more erosion and weathering along these planes, which creates greater water storage capacity and infiltration for water. However, without more information about relative permeabilities of these rock types, it is unclear whether these differences caused the observed pattern. Furthermore, Leopold et al., (2013) found that bedrock outcrops in this catchment create a heterogeneous landscape that alternates between pockets of soil and bedrock; this could possibly create some areas of bedrock with little to no flowpath connection and other areas of soil with a continuous flowpath connection to the stream.



Figure 23. An example of a log jam at MU where water was dammed behind the log and resurfaced a meter downstream from the log jam. Left picture shows the flowing water before the log and dry channel after the log. Right picture shows resurfaced water downstream.

MU's drainage class is described as somewhat excessively drained' (Soil Survey Staff, 2017).

Drainage class refers to the frequency and duration of wet conditions similar to those under which the soil formed. The drainage class could be another explanation as to why streamflow in this catchment is spatially discontinuous because an excessively drained soil will not hold water long, resulting in dry areas. Small dams created by logs would result in <1 m dry segments in the stream below the dam (Figure 22). At the confluence of the two main tributaries, the stream was also dry. Because this area is a large open flat area, the water became dispersed rather than concentrated, and this may have caused the local channel drying (Figure 23).

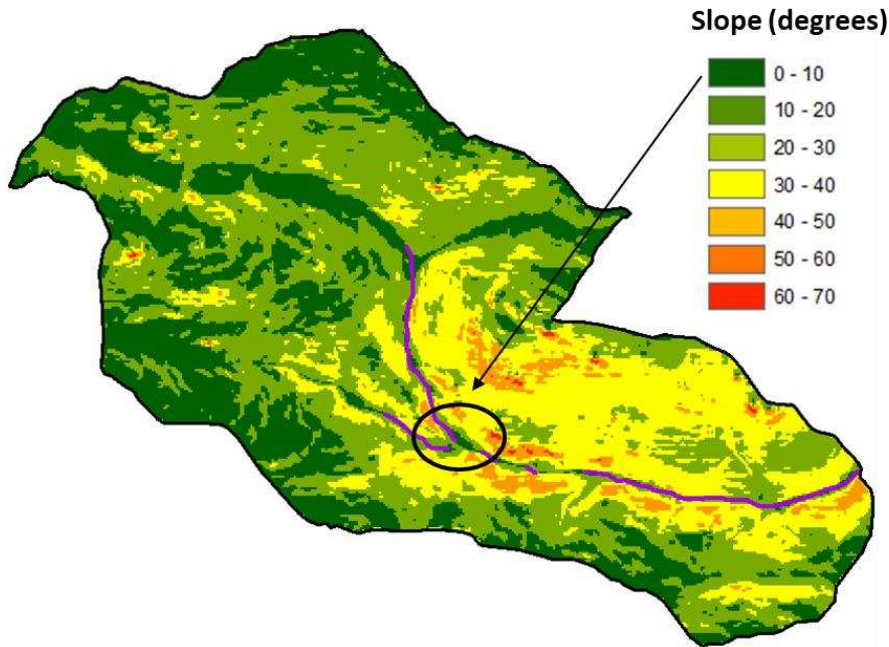


Figure 24. Flat open area along MU (Gordon) channel valley is dry.

5.4. Upper (U)

U, the highest elevation site, flowed year around and had a short rising limb but long falling limb. U had the greatest precipitation and longest snow persistence (SP), which provides high storage of water during the winter and spring. The falling limb is long lasting because the snowpack and subsurface storage zones slowly release water over the summer. U's first visit still had snow on the higher elevations, so flow was only observed on the lower elevations. By the second trip the flowing portion of the stream had moved upstream as the snow melted. In addition, the first trip had greater discharge than the second trip. It is possible that the snow pack was supplying the greater discharge during the first trip, and when the snow melted this supply was gone and therefore discharge decreased. Surface channel flow was discontinuous along the talus and rubble and continuous over the sandy soil in the lowlands (Figure 18d(8)). The talus is highly porous and heterogeneous and is classified as 'somewhat excessively

drained' (Soil Survey Staff, 2017). Therefore, flow could move easily into and out of the subsurface, leading to the stream infiltrating and exfiltrating in some locations depending on porosity and topography. MU and U both had spatially disconnected stream networks and were classified as 'somewhat excessively drained'; this suggests that where the water infiltrates or drains very easily can create a discontinuous stream network. U's watershed also contains the largest water capacity (350 cm/cm) relative to the other watersheds due to the talus and till (Soil Survey Staff, 2016). This gives the watershed the greatest storage capacity to hold water, which, in addition to long lasting snow could contribute to its year-round flow.

Overall, the assessments of how stream networks compare to geology and soils are qualitative and rely on relatively coarse information on rock and soil types. Future research could incorporate more field measurements of bedrock types, fracture and joint patterns, and soil type to enable more quantitative analysis of how geology and soils relate to streamflow patterns.

5.5. Topography

Topographic algorithms are useful for mapping streams because incised channels can be detected from topography. However, headwaters are dynamic features and are not only influenced by topography but also by the surrounding geology, soil and vegetation; therefore, these topographic algorithms may not be 100% accurate.

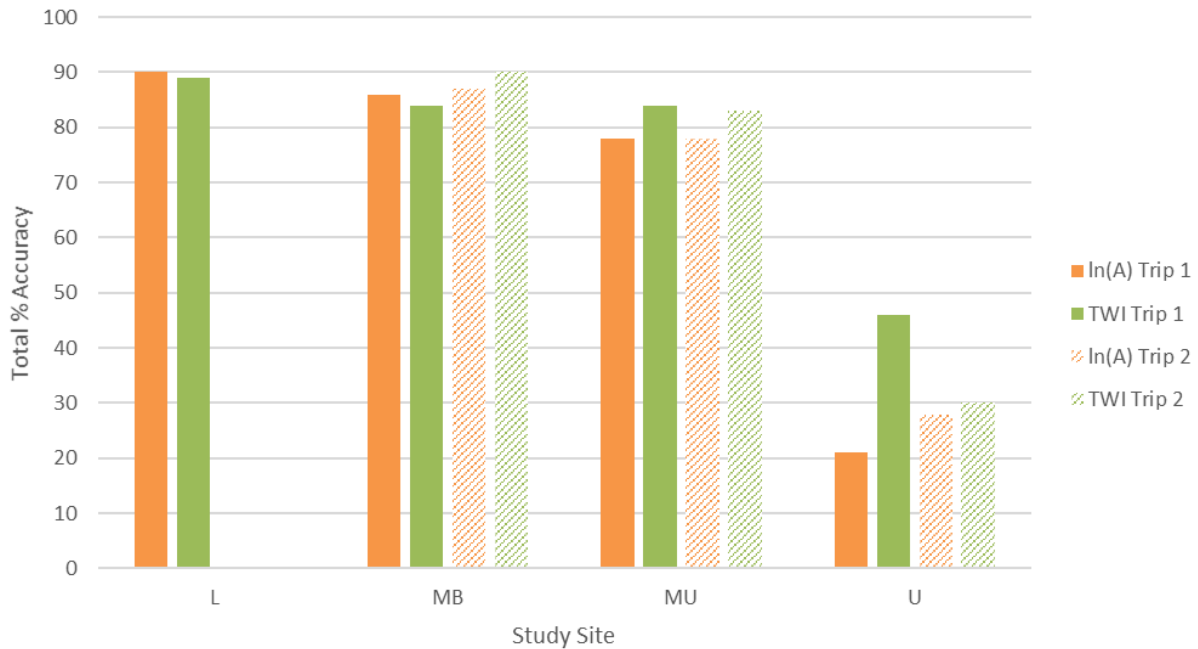


Figure 25. Total % accuracy of each 10 m topographic index for mapping surface flow locations at every study site.

The performance of indices varied between sites and between DEM resolutions but overall performed reasonably well (73 – 91%) except for U (21 – 73%). This agrees with Hastings (2012) who found that flow accumulation and TWI produce acceptable channel networks given the appropriate thresholds and DEM resolution. TWI and In(a) varied by 0-25% total accuracy, 0-25% FP, and 0- 15% FN depending on which site and what DEM. The only significant differences (>5%) between In(a) and TWI performance metrics were at the higher elevation sites, MU and U, where TWI performed 6-25% better for total accuracy, except for MU with 1 m. When TWI performs better, this is an indication that local slope is important for determining stream location. Because In(a) and TWI performed well, and TWI performed slightly better at MU and U, our results agree with Güntner et al., (2004) who found that UAA was the single most important factor explaining saturated areas but the addition of slope in TWI leads to improved accuracy. U has the largest mean slope relative to the other sites, so better performance of TWI

there may indicate that slope plays a larger role in stream location at sites with steep hillslopes. This could be because the higher the slope the less likely surface flow will initiate. Flow will instead stay below the ground surface, except in areas where the local slope flattens. Prior research has found evidence of shallow subsurface flow that exfiltrates in flat areas to produce saturation excess overland flow in this catchment (Kampf et al., 2015). At MU, which also has better performance with TWI, shallow subsurface flow can also develop on the north-facing slopes (Hinckley et al., 2014); however, in contrast to U, this catchment has the lowest overall slope, suggesting that slope not the primary indicator of surface flow locations.

The performance of TWI and $\ln(a)$ were not consistent over time. The thresholds generally estimated stream networks adequately in the first survey but poorly predicted the stream networks for the second survey. The first survey was earlier in the snow melt season, and both stream discharge and stream lengths were longer. The second survey was about a month after the first survey, when discharge was lower and stream lengths decreased. The poorer performance of topographic algorithms during the second trip is similar to the findings of Stieglitz et al. (2003), who found that there is high correlation between TWI and water table depths when the soils are wet and much less so during the dry conditions. Rodhe and Seibert (1999) suggest that TWI is a method that presents the extreme end of the wetness spectrum, so this could be why TWI is not as effective for mapping flowing channel locations as the watershed dries. Another possibility is that other factors besides topography have greater influence on stream location during lower flows, similar to the findings of Jensco and McGlynn (2011) and Emanuel et al. (2014), who showed that the relative influences of topographic,

vegetative, and geologic controls on streamflow and catchment connectivity can change through time with catchment wetness states. My results agree with this finding because the topographic indices performed worse during the second survey (with lower discharge) and geology/soil explained most of the mismatch between the observed and predicted stream network during the drier second surveys. Another observation I made with low discharge at these sites was that pools and dry channel segments were common because the flow was not high enough to be sustained when it encountered more porous substrate, had divergent flow paths in flat topography (Figure 23), and encountered natural 'dams' created by sediment and fallen logs (Figure 22).

Channel head locations were also not represented well by topographic thresholds. Only 18 of 214 channel initiation locations were correctly identified from all the channels produced from TWI and $\ln(a)$ for both trips and DEM resolutions. Inaccurate prediction and overprediction of channel heads by topographic indices is a common issue (Orlandini et al., 2003; Hastings, 2012). Other studies used an inverse relationship between contributing drainage area and the local valley slope, to choose a threshold to derive geomorphic channel heads and channels (e.g. Horton, 1945; Montgomery and Dietrich, 1989; Wilgoose et al., 1991; Kirkby, 1988; Dietrich et al., 1993; Ijjasz-Vasquez and Bras, 1995). However, our findings highlight the variability in flow initiation locations, which are not predictable from topography alone.

DEM resolution had inconsistent effects on derived channel accuracy, which agrees with findings that terrain indices have high sensitivity to elevation data resolution and result in

varying values (McMaster, 2002; Sørensen and Seibert, 2007; Vaze et al., 2010; Orlandini et al., 2011; Hastings and Kampf, 2014). 1 m performed significantly better at U, but only slightly better at MB. 1 m and 10 m performed similarly at L, whereas at MU, 1 m did slightly better for the first trip, and 10 m did slightly better for the second trip. It is possible that the finer resolution is able to capture the microtopography along the channel bed, which was needed for U (which is the steepest site) to represent its discontinuous flow paths and the local slope effects on developing saturation overland flow. For U specifically, this could demonstrate that microtopography may be more important for channel network development in rugged and steep landscapes (Hastings, 2012). Kienzle et al., (2004) also found that areas with steeper terrain needed higher resolution, whereas the flatter the terrain the coarser the DEM that can be used. Because at all other sites differences between performance for 1 m and 10 m DEMs was minor (<11%), there is no strong reason to choose one or the other. These findings agree with previous studies that suggest the optimum grid cell size should range from 1 m to 10 m for creating terrain derivatives (Kienzle, 2004; Colson, 2006; Deng et al., 2007), but disagrees with studies that claim 10 m resolution is best because it reduces the confounding effects of microtopography (Jensco et al., 2009; Grabs et al., 2009).

Another resolution issue that can arise from comparing mapped stream data and terrain variables is the difference in resolution between the DEM and the GPS, which can create misalignment of a feature position (Figure 25). Higher resolution data is found to capture geomorphic characteristics better and enhance the accuracies of derived channel networks while lower resolution may overgeneralize (Erskine et al., 2006; Vaze et al., 2010; McMaster,

2002). Despite these uncertainties, UAA and TWI still identified channel locations reasonably well, using the channel buffer to account for the GPS accuracy. Sørensen and Seibert (2007) also suggested that optimal DEM resolution size should be chosen based landscape scale and the length of topographic features, which will vary between sites. A study that compares various stream sizes and DEM resolution would be insightful for this issue.

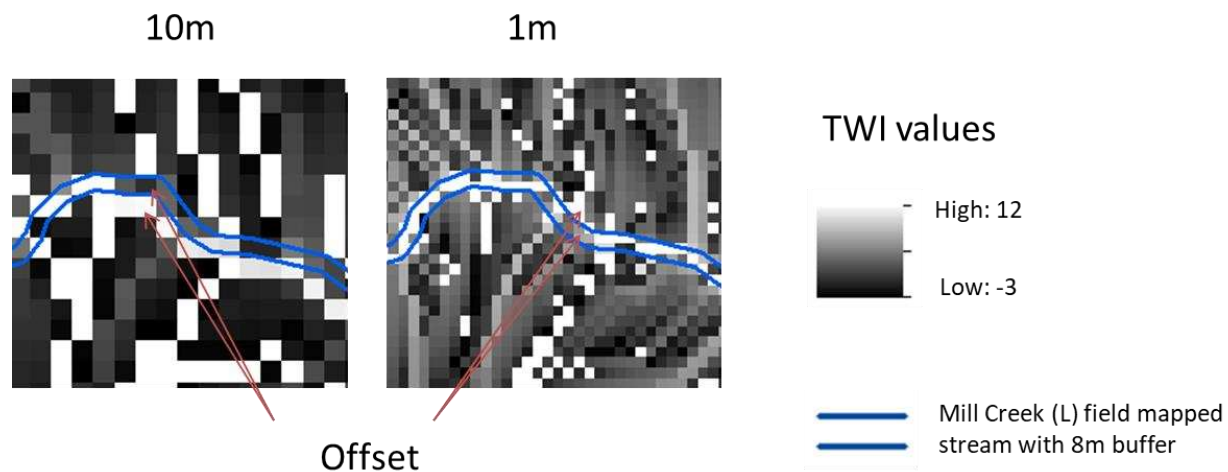


Figure 26. Resolution of DEMs (10 m or 1 m) and GPS mapped stream (5-8m): a) a snapshot of 1 m TWI of L (Mill Creek) and the digitized stream shows that they are slightly offset.

Overall this study demonstrated that topographic thresholds for surface flow initiation and surface channel networks are not consistent between catchments, DEM resolutions, and time of year. The amount a stream expands and contracts will affect how much the thresholds will vary at a given location. For both the TWI and contributing area ($\ln(a)$) along with all the other terrain indices, thresholds must be specified by the user, and the value that is chosen strongly affects the location of the predicted channel heads (Helminger et al., 1993; Heine, 2004; Clubb et al, 2014). Although the topographic thresholds from this study produce a power law relationship between stream density and accumulation area (Figure 26) that is consistent with other studies (e.g. (Montgomery Dietrich, 1989; Tarboton et al., 1991; Helminger et al., 1993), it

is important to consider that every watershed will have a unique relationship between threshold and stream density (Figure 11). Therefore, an “optimal” threshold may not exist for an entire study region because thresholds for channel head locations vary within a given landscapes and across different landscapes (Fotheringham, 1997; Li and Wong, 2010; Kampf and Mirus, 2013). Our results show that headwater systems need multiple thresholds for different elevation/climate zones and that the thresholds will vary throughout the year. This agrees with many researchers that warn against using fixed drainage networks in hydrologic models, as they fail to describe the dynamic nature of surface flow in channels (Wharton, 1994; Burt and Butcher, 1986).

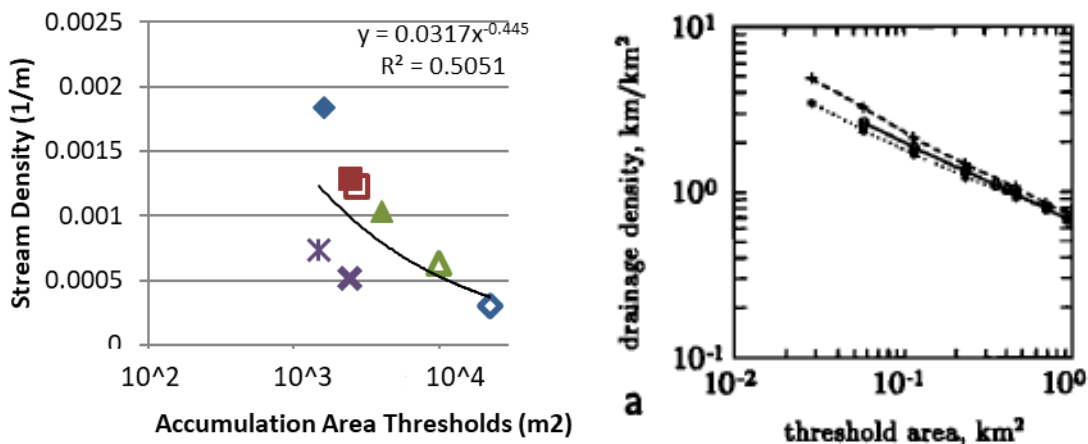


Figure 27. Linear relationship between $\ln(a)$ and stream density at the study catchments (left) compared with Helmlinger et al. (1993) catchments from New York, California, and Idaho.

The contributing area threshold values for the study catchments range between 148,000 m² (at U, highest elevation site) – 2,467,900 m² (at L, lowest elevation site). The highest value is so large because it is for the lowest elevation when it was drying up. Without the drying L threshold, the largest contributing area threshold is 989,700 m² (at MU, middle unburned site). These values are somewhat larger than what studies have found for the Colorado Front range,

where Henkle (2011) found thresholds for channel heads to be a range of 10,000 m² -600,000 m² and an average of 108,258 m², and Hastings (2012) used 129, 372 m² as the optimum threshold for Loch Vale, which includes U. Other studies found various ranges in different regions such as 500 m² - 10,000 m² in the Italian Alps (Orlandini et al., 2011), 637 m² - 60,978 m² in Washington state (Jaeger et al., 2007), 1,000 m² – 1,000,000 m² in coastal Oregon (Montgomery and Dietrich, 1992), 7,000 m² - 800,000 m² across California (Montgomery and Dietrich, 1992), and 8,000 m² - 300,000 m² in Tennessee (Montgomery and Foufoula- Georgiou, 1993). The thresholds for the study region overall are on the larger side of these ranges of values, which is consistent with Montgomery and Dietrich's (1989) finding that semiarid climates have larger threshold areas than humid regions. However, comparing the catchments to one another in the study area, the wetter sites actually have higher flow initiation thresholds than the drier sites.

5.6. Vegetation and Aspect

From qualitative analysis, vegetation types did not appear to affect the stream location or duration, but instead the site elevation, aspect, and slope influenced what vegetation type existed in each watershed. The vegetation map from NLCD is too coarse and inaccurate to use for comparing stream channel locations to vegetation type. Even though no trends were found, vegetation plays an active role in the redistribution process of water through evapotranspiration, preferential flow, plant uptake, interception and an accumulation effect on water yield (Laio et al., 2001; Kampf and Mirus, 2013; Emanuel et al., 2014; Davie and Fahey,

2005). More detailed vegetation mapping would be needed to connect this to stream surface flow patterns.

In mountain catchments, aspect could be an overarching factor influencing the hydrological cycle, however from qualitative analysis no trends were found between stream flow intermittence and aspect in this study. Hastings, (2012) also did not find any correlation between the TWI and $\ln(a)$ values at channel heads and aspect. Prior research indicates that hillslopes with different aspects have different microclimates and soil moistures, where north-facing slopes are more hydrologically connected and south facing slope soils experience more drying (Kelly, 2012; Hinckley et al., 2014). This was not reflected in the spatial distribution of streamflow at MU or any other site, although possibly a connection could be identified with a more quantitative analysis of aspect.

5.7. The overarching effects of climate/elevation

Elevation is correlated with increased SP, precipitation, and decreased temperature in the study region which is consistent with other studies (Richer, 2009; Moore, 2012; Richer et al., 2013).

TWI and $\ln(a)$ thresholds also generally increased with elevation (Figure 16), a finding that contrasts with previous studies that found higher elevation streams are associated with smaller upland contributing drainage areas (Schumm, 1979; Villines et al., 2015) and that humid regions require small contributing areas for runoff generation than drier regions (Montgomery and Dietrich, 1988). With all other factors equal, I would expect greater stream density (smaller TWI and $\ln(a)$ values) in areas with high precipitation; however, this is not what was found in this

study. While higher precipitation increased flow duration and discharge (Figure 12b, c), precipitation did not have a strong correlation with stream density (Figure 12a), which indicates that higher precipitation does not necessarily mean greater spatial extent of surface water. The decrease in stream density in the wetter catchments likely relates to deeper soils and more subsurface storage. At the wettest site, U, high snow accumulation and water storage in the talus and rock glacier not only supply year-round water but with the addition of high slopes also creates subsurface flowpaths resulting in a smaller stream density.

Dry areas (L, MB) do not have much evidence of shallow subsurface flow; rather flow emerges from fracture or fault zones. At L, this fracture flow is not large enough to sustain flow year-round, so when the flow stops delivering water to the channel network, almost the entire network dries, except for areas with less permeable bedrock (trondhjemite) and greater soil water retention. At MB decreased forest transpiration from the 2012 fire may have led to greater subsurface flow, which is sustained throughout the year in consistent locations. In contrast, MU, which has about the same mean annual precipitation as MB, has both groundwater and soil water contribution (Heckman, 2012), and interfaces between soil pockets and bedrock outcrops influences the channel surface flow locations (Leopold et al., 2013). There are also more opportunities for the surface flow to infiltrate into deep soils; at MU, the catchment is very responsive to rain, even after the channel has dried, indicating that the subsurface stays relatively wet.

5.8. Landscape evolution

The observation that streams that preferred following faults, shear zones, bedding contacts, and more erodible/resistant rock (schists, sandstones) types and usually circumvented resistant rock types (granites, pegmatites) could be the consequence of landscape evolution processes. Mountainous headwater catchments are formed from tectonic uplift and channels incising through rocks to shape the topography. A rock's tensile strength determines the speed of its erosion rates; tensile strength has an inverse relationship with erosion rates (Sklar and Dietrich, 2001), giving rock types like igneous (granites), metamorphic rocks (metasandstone, quartzite, andesite) lower erosion rates than sedimentary rocks (sandstone, mudstone, limestone). As an extension to this, my results suggest that over time the strength/resistance of different rock types to erosion can influence the locations of channel incision. Glacial processes affected the highest elevation site, where talus and rubble cover the high elevations of the catchment. These boulder sized particles create a heterogeneous landscape with high storage capacity, which lead to a spatially discontinuous stream and more limited drainage network development than in the lower elevation unglaciated catchments.

5.9 Uncertainties

Several uncertainties affect the analyses in this study. The environmental factors that were compared to the observed stream varied in resolution and were coarser than the resolution of the digitized observed stream. The digitized stream had a resolution of less than 10 m while the derived streams have 8 m (1 m buffered to 8 m) and 10 m resolution. The vegetation dataset has a 30 m resolution and soil has 10 m or 30 m depending on the map. Geology has a

1:24,000 scale where 1 cm on the map represents 200 m, and NHD has a range of scale between 1:12,000 to 1:63,000. Comparing these data to the less than 10 m streams will come with uncertainty about stream locations and associated vegetation or rock type. The hydraulic conductivities will vary between rock types and even within a single rock type when there are joints, fractures, or foliations that increase hydraulic conductivity. This can affect where streams will flow because of the varying hydraulic conductivities, but such fine-scale information is not available in the geologic maps. The shape of the drainage basin can also affect the timing and magnitude of discharge which could possibly affect streamflow locations. Because the surveys were taken during different times for each site, this will affect results of this study that compare discharge and drainage densities between watersheds. The lower site is most affected by this because it changed stream length drastically in a month, whereas the middle elevation sites, MU and MB, did not change much, and U changed because of the melting of snow. If the surveys had been conducted at different times of year or during years with higher or lower precipitation, the thresholds for streamflow initiation would likely have been different. Ongoing research mapping these patterns can help clarify the magnitude of spatial and temporal variability in these surface flow patterns over longer time periods. For example, future research could focus on one watershed and map the stream networks every week to improve the understanding of how the stream networks changes through time as the discharge changes.

5.10 Conceptual Model and Future Considerations

Based on my findings in this study, I developed conceptual models describing the.... effects of geology and soil on streamflow locations. During surveys with lower flows, the hydraulic

conductivities of soils and bedrocks highly influenced streamflow location and duration. Where streams crossed over soils/bedrock with higher conductivity the water infiltrated, leading to discontinuous surface flow (Figure 28a). When streams had higher flows, this effect was not observed (Figure 28b).

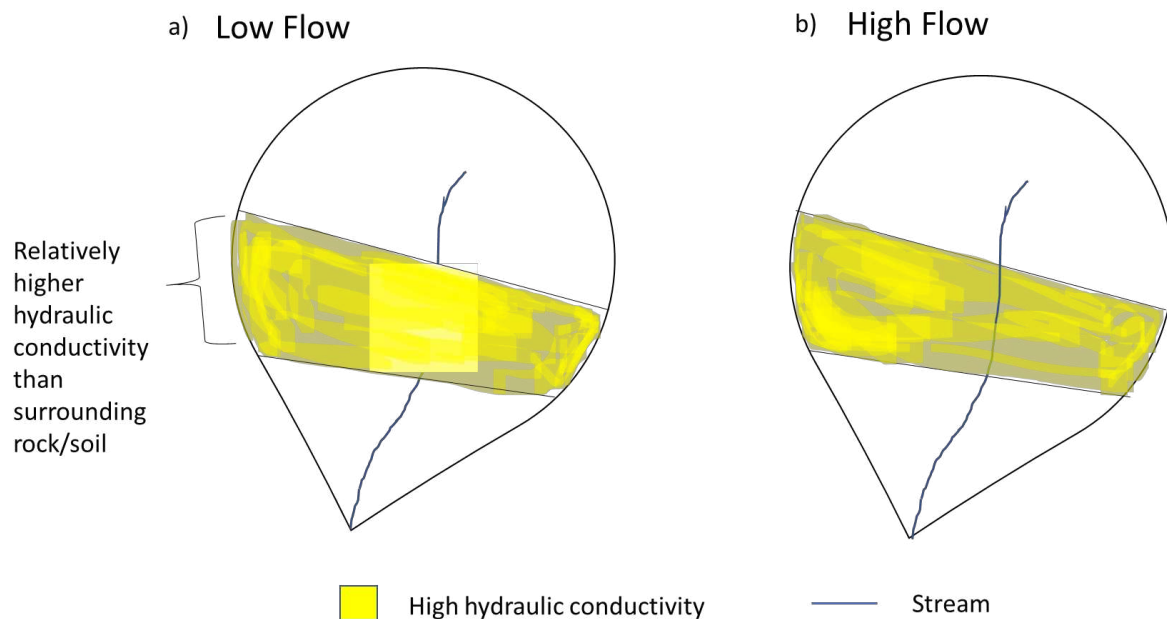


Figure 28. Conceptual model showing the effects of relative hydraulic conductivity on surface channel flow depending on the magnitude of flow. a) When stream has lower flow the effects of the lithology and soil types is greater, where flow infiltrates in areas of higher hydraulic conductivity. b) When stream has higher flow, lithology/soil has less of an effect on streamflow location.

The permeability of the bedrock types can also affect the stream location. More impermeable rocks (low hydraulic conductivity) are harder to erode by small streams, so the streams will go around those rock types (Figure 29a). Also bedding contacts, faults and shear zones are more erodible, so streams will prefer to flow along them (Figure 29a,b)

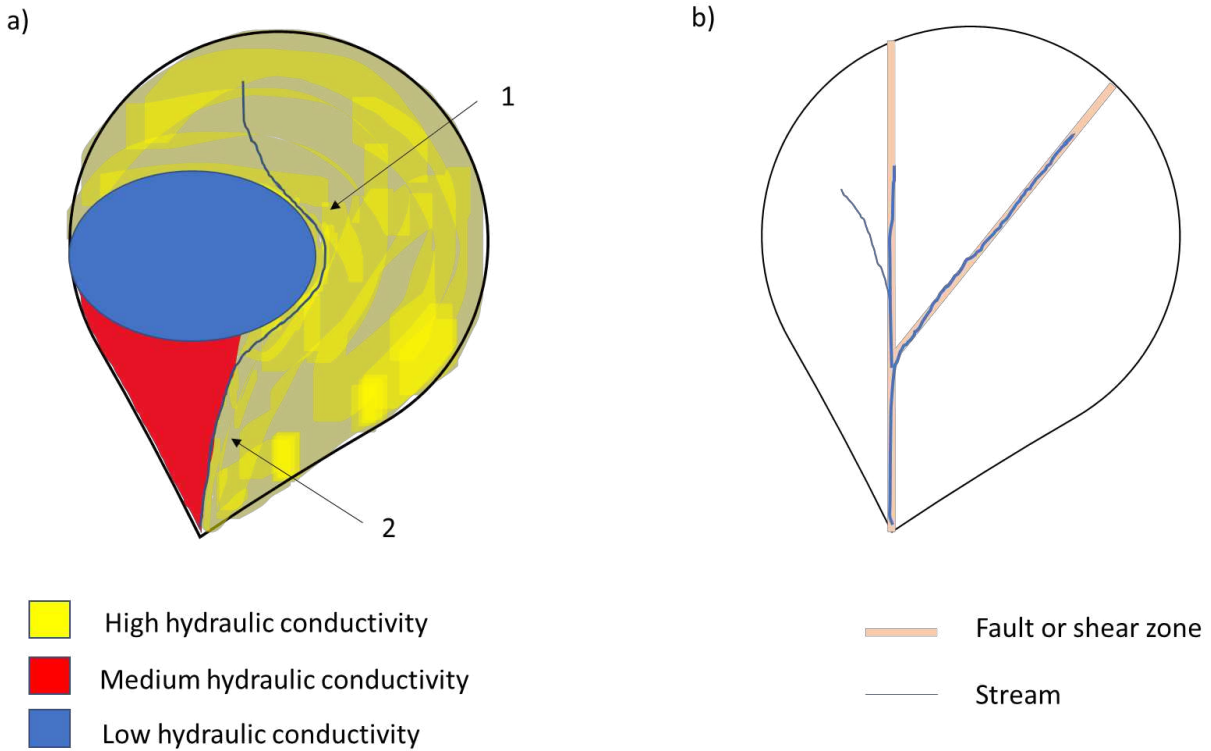


Figure 29. Conceptual model showing the effects of bedrock hydraulic conductivity and structural geology on streamflow location. a) Small streams go around bedrock with lower hydraulic conductivities and prefer to flow on bedrocks with higher hydraulic conductivities (1). Stream also prefers to flow along bedding contacts (2). b) Stream flows along faults or shear zones because they are more easily erodible.

Because the hydraulic conductivities of the soil and geology affect the streamflow locations, one option for improving channel delineation would be to include hydraulic conductivities in the topographic indices, UAA and TWI. For example, this could involve creating a rating of the hydraulic conductivities from 1 to 10, where 1 is lowest hydraulic conductivity and 10 is the highest hydraulic conductivity. This value could then be multiplied by the UAA and TWI so that the increase in hydraulic conductivities would increase the UAA and TWI and increase wetness . During low flow times of year, higher hydraulic conductivity can cause loss of surface flow to the subsurface, so the weighting scheme could change to give higher weight to low hydraulic conductivity. Therefore, an algorithm to map surface flow extent with topography and

hydraulic conductivity could also include a hydrograph simulation and variable stream networks depending on the time of year and the overall discharge.

6. CONCLUSIONS

My research explored how the spatial and temporal variability of streamflow relates to topography and other catchment characteristics across a gradient ranging from a low elevation intermittent snow catchment to a glaciated high elevation catchment. The lowest elevation stream had the largest stream density early in the season, but it dried up quickly in the summer and ended with the lowest stream density. Counter to expectations of increasing stream density with wetter climates at higher elevations, stream densities generally declined with elevation, possibly because greater soil development and subsurface storage capacity in wetter sites limited surface water flow and channel network development.

Topographic thresholds for channel initiation varied across sites and over time within each site. The thresholds increased with increasing elevation except for the highest elevation site, which decreased. These thresholds were 73 – 91% accurate in mapping surface flow locations with the exception of U which had poor accuracy of 21 – 73% because it is a glacial catchment and could be driven by subsurface flow and subsurface bedrock topography below the talus. TWI performed better at MU and U with a 6-25% increased total accuracy but generally they performed closely. The derived channels were inaccurate in areas with spatially discontinuous flow, where the surface geology and soil texture may have caused localized infiltration and exfiltration of water. Some of the errors in topographically derived channel networks also related to areas where the permeability and erodibility of geology/soils affected stream location. Geologic structure also affected stream flow locations, as many streams flowed over

faults, shear zones and bedding contacts. These faults also acted as conduits of groundwater, supplying water to the streams.

Based on these findings results, I suggest incorporating geologic and soil hydraulic conductivity and erodibility information into future channel delineation methods. The information I compiled can also be used to help determine how topographic thresholds for surface flow initiation relate to elevation, discharge, stream density and other factors. This type of information would immensely improve stream channel maps, which are difficult to produce in detail everywhere because of the limitations of time, cost and equipment for conducting detailed stream mapping.

REFERENCES

- Ali, G., Birkel, C., Tetzlaff, D., Soulsby, C., McDonnell, J.J. and Tarolli, P., 2014. A comparison of wetness indices for the prediction of observed connected saturated areas under contrasting conditions. *Earth Surface Processes and Landforms*, 39(3), pp.399-413.
- Anderson, M.G. and Burt, T.P., 1978. The role of topography in controlling throughflow generation. *Earth Surface Processes and Landforms*, 3(4), pp.331-344.
- Benstead, J.P. and Leigh, D.S., 2012. An expanded role for river networks. *Nature Geoscience*, 5(10), pp.678-679.
- Band, L.E., 1986. Topographic partition of watersheds with digital elevation models. *Water resources research*, 22(1), pp.15-24.
- Beven, K. and Kirkby, M., 1979. A physically based variable contributing area model of basin hydrology. *Hydrology Science Bulletin* 24(1):43–69.
- Beven, K. and Wood, E.F., 1983. Catchment geomorphology and the dynamics of runoff contributing areas. *Journal of Hydrology*, 65(1), pp.139-158.
- Beven, K., 1987. Towards the use of catchment geomorphology in flood frequency predictions. *Earth Surface Processes and Landforms*, 12(1), pp.69-82.
- Beven, K. and Freer, J., 2001. A dynamic topmodel. *Hydrological processes*, 15(10), pp.1993-2011.
- Brogan, D. J., Nelson, P. A., and MacDonald, L. H. (2017) Reconstructing extreme post-wildfire floods: a comparison of convective and mesoscale events. *Earth Surf. Process. Landforms*, 42: 2505–2522.
- Braddock, W.A., Calvert, R.H., O'Connor, J.T. and Swann, G.A., 1989. Geologic map of the Horsetooth Reservoir quadrangle, Larimer county, Colorado (No. 1625).
- Braddock, W.A. and Cole, J.C., 1990. Geologic map of Rocky Mountain National Park and vicinity, Colorado (No. 1973).
- Burns, D.A., Murdoch, P.S., Lawrence, G.B. and Michel, R.L., 1998. Effect of groundwater springs on NO₃⁻ concentrations during summer in Catskill Mountain streams. *Water Resources Research*, 34(8), pp.1987-1996.
- Burt, T.P. and Butcher, D.P., 1986. Development of topographic indices for use in semi-distributed hillslope runoff models. *Geomorphology and Land Management*, 58, pp.1-19.

Childers, H.M., M.E. Passmore, and L.J. Reynolds, 2006. Extent of Headwater Perennial and Intermittent Streams. Center for Educational Technologies, Wheeling Jesuit University, Wheeling, West Virginia.

Clow, D. W., L. Schrott, R. Webb, D. H. Campbell, A. Torizzo, and M. Dornblaser (2003), Ground water occurrence and contributions to streamflow in an alpine catchment, Colorado Front Range, *Groundwater*, 41(7), 937–950, doi:10.1111/j.1745-6584.2003.tb02436.x.

Clubb, F.J., Mudd, S.M., Milodowski, D.T., Hurst, M.D. and Slater, L.J., 2014. Objective extraction of channel heads from high - resolution topographic data. *Water Resources Research*, 50(5), pp.4283-4304.

Colson, T.P., 2006. Stream Network Delineation from High Resolution Digital Elevation Models. Ph.D. Dissertation, Department of Forestry and Environmental Resources, North Carolina State University, Raleigh, North Carolina.

Colson, T., J. Gregory, J. Dorney, and P. Russell, 2008. Topographic and Soil Maps Do Not Accurately Depict Headwater Stream Networks. *National Wetlands Newsletter* 30:25-28.

Costa-Cabral, M.C. and Burges, S.J., 1994. Digital elevation model networks (DEMON): A model of flow over hillslopes for computation of contributing and dispersal areas. *Water resources research*, 30(6), pp.1681-1692.

Cote et al., 2009. A new measure of longitudinal connectivity for stream networks, *Landscape Ecology* 24(2):101-113.

Datry, T., Larned, S.T. and Tockner, K., 2014. Intermittent rivers: a challenge for freshwater ecology. *BioScience*, 64(3), pp.229-235.

Davie, T. and Fahey, B., 2005. Forestry and water yield-current knowledge and further work. *New Zealand Journal of Forestry*, 49(4), pp.3-8.

Deilami, B.R., Al-Saffar, M.R.A., Sheikhi, A., Bala, M.I. and Arsal, D., 2013. Comparison of surface flows derived from different resolution DEM. *Int J Eng Technol IJET-IJENS*, 13, pp.82-85. *International Journal of Engineering and Technology*

Deng, Y., Wilson, J.P. and Bauer, B.O., 2007. DEM resolution dependencies of terrain attributes across a landscape. *International Journal of Geographical Information Science*, 21(2), pp.187-213.

Di Luzio, M., Srinivasan, R., and Arnold, J. G., 2002. Integration of watershed tools and SWAT model into BASINS. *Journal of American Water Resource Association*, 38(4), 1127–1141.

Dietrich, W.E., Wilson, C.J., Montgomery, D.R. and McKean, J., 1993. Analysis of erosion thresholds, channel networks, and landscape morphology using a digital terrain model. *The Journal of Geology*, 101(2), pp.259-278.

Dodds, W.K., Oakes, R.M., 2006. Controls on nutrients across a prairie stream watershed: land use and riparian cover effects. *Environ. Manage.* 37, 634–646.

Dodds, W.K., Oakes, R.M., 2008. Headwater influences on downstream water quality. *Environ. Manage.* 41, 367–377.

Dowman, C.E., Ferré, T., Hoffmann, J.P., Rucker, D.F. and Callegary, J.B., 2003. Quantifying ephemeral streambed infiltration from downhole temperature measurements collected before and after streamflow. *Vadose Zone Journal*, 2(4), pp.595-601.

Duan J, Miller NL. 1997. A generalized power function for the subsurface transmissivity profile in TOPMODEL. *Water Resources Research* 33(11): 2559–2562.

Dunne, T. and Black, R.D., 1970. Partial area contributions to storm runoff in a small New England watershed. *Water resources research*, 6(5), pp.1296-1311.

Emanuel, R.E., Hazen, A.G., McGlynn, B.L. and Jencso, K.G., 2014. Vegetation and topographic influences on the connectivity of shallow groundwater between hillslopes and streams. *Ecohydrology*, 7(2), pp.887-895.

Ersine, R.H., Green, T.R., Ramirez, J.A. and MacDonald, L.H., 2006. Comparison of grid-based algorithms for computing upslope contributing area. *Water Resources Research*, 42(9).

Esri. "Geographic" [Basemap]. "National Geographic World Map".
<http://www.arcgis.com/home/item.html?id=b9b1b422198944fbbd5250b3241691b6>

Esri. "Imagery" [Basemap]. "World Imagery".
<http://www.arcgis.com/home/item.html?id=10df2279f9684e4a9f6a7f08febac2a9>

Fisher, S.G., Sponseller, R.A. and Heffernan, J.B., 2004. Horizons in stream biogeochemistry: flowpaths to progress. *Ecology*, 85(9), pp.2369-2379.

Fotheringham, A. S., 1997. Trends in quantitative methods I: Stressing the local. *Progress in Human Geography*, 21, 88–96.

Fritz, K., E. Hagenbuch, E. D'Amico, M. Reif, P. Wigington, S. Leibowitz, R. Comeleo, J. Ebersole, and T. Nadeau, 2013. Comparing the Extent and Permanence of Headwater Streams from Two Field Surveys to Values from Hydrologic Databases and Maps. *Journal of the American Water Resources Association* 49:867-882.

Gable, D.J., 1980. Geologic map of the Gold Hill quadrangle, Boulder County, Colorado (No. 1525).

Gallant, J.C. and Wilson, J.P., 1996. TAPES-G: a grid-based terrain analysis program for the environmental sciences. *Computers & Geosciences*, 22(7), pp.713-722.

Goodrich, D.C., Williams, D.G., Unkrich, C.L., Hogan, J.F., Scott, R.L., Hultine, K.R., Pool, D., Coes, A.L., Miller, S., 2004. "Comparison of methods to estimate ephemeral channel recharge, walnut gulch, san pedro river basin, Arizona". *Groundwater Recharge in a Desert Environment: The Southwestern United States*. Water Sci. Appl. Ser. 9, 77–99.

Grabs, T., Seibert, J., Bishop, K. and Laudon, H., 2009. Modeling spatial patterns of saturated areas: A comparison of the topographic wetness index and a dynamic distributed model. *Journal of Hydrology*, 373(1), pp.15-23.

Güntner, A., Seibert, J. and Uhlenbrook, S., 2004. Modeling spatial patterns of saturated areas: An evaluation of different terrain indices. *Water Resources Research*, 40(5).

Hammond, J. C., F. A. Saavedra, S. K. Kampf (2017). MODIS MOD10A2 derived snow persistence and no data index for the western U.S., HydroShare, <http://dx.doi.org/10.4211/hs.1c62269aa802467688d25540caf2467e>

Hansen, W.F., 2001. Identifying Stream Types and Management Implications. *Forest Ecology and Management* 143:39-46

Hastings B., 2012. Comparison of digital terrain and field-based channel derivation methods in a subalpine catchment, Front Range, Colorado. MS Thesis, Colorado State University, Fort Collins, CO.

Hastings, B.E. and Kampf, S.K., 2014. Evaluation of digital channel network derivation methods in a glaciated subalpine catchment. *Earth Surface Processes and Landforms*, 39(13), pp.1790-1802.

Heath, R.C., 1983. Basic ground-water hydrology (Vol. 2220). US Geological Survey.

Heckman, C., 2012. Springs of Gordon Gulch: A Groundwater Analysis. Honors Thesis, Colorado University, Boulder, CO.

Heine, R.A., Lant, C.L. and Sengupta, R.R., 2004. Development and comparison of approaches for automated mapping of stream channel networks. *Annals of the Association of American Geographers*, 94(3), pp.477-490.

Helmlinger, K.R., Kumar, P. and Fofoula-Georgiou, E., 1993. On the use of digital elevation model data for Hortonian and fractal analyses of channel networks. *Water Resources Research*, 29(8), pp.2599-2613.

Henkle, J.E., Wohl, E. and Beckman, N., 2011. Locations of channel heads in the semiarid Colorado Front Range, USA. *Geomorphology*, 129(3-4), pp.309-319.

Hinckley, E.L.S., Ebel, B.A., Barnes, R.T., Anderson, R.S., Williams, M.W. and Anderson, S.P., 2014. Aspect control of water movement on hillslopes near the rain–snow transition of the Colorado Front Range. *Hydrological Processes*, 28(1), pp.74-85.

Hjerdt, K.N., McDonnell, J.J., Seibert, J. and Rodhe, A., 2004. A new topographic index to quantify downslope controls on local drainage. *Water Resources Research*, 40(5).

Homer, C.G., Dewitz, J.A., Yang, L., Jin, S., Danielson, P., Xian, G., Coulston, J., Herold, N.D., Wickham, J.D., and Megown, K., 2015, Completion of the 2011 National Land Cover Database for the conterminous United States—Representing a decade of land cover change information. *Photogrammetric Engineering and Remote Sensing*, v. 81, no. 5, p. 345-354

Horton, R.E., 1945. Erosional development of streams and their drainage basins; hydrophysical approach to quantitative morphology. *GSA Bulletin*, 56(3), pp.275-370.

Ijjasz-Vasquez, E. and Bras, R. (1995), Scaling regimes of local slope versus contributing area in digital elevation models. *Geomorphology*, 12(4), 299-311.

Iorgulescu I, Musy A. 1997. Generalisation of TOPMODEL for a power law transmissivity profile. *Hydrological Processes* 11: 1353–1355.

Jaeger, K.L., Montgomery, D.R. and Bolton, S.M., 2007. Channel and perennial flow initiation in headwater streams: management implications of variability in source-area size. *Environmental Management*, 40(5), p.775.

Jaeger, K.L., and Olden, J.D., 2011, Electrical resistance sensor arrays as a means to quantify longitudinal connectivity of rivers, *River Research and Applications*, doi:10.1002/rra.1554.

Jencso, K.G., McGlynn, B.L., Gooseff, M.N., Wondzell, S.M., Bencala, K.E. and Marshall, L.A., 2009. Hydrologic connectivity between landscapes and streams: Transferring reach-and plot-scale understanding to the catchment scale. *Water Resources Research*, 45(4).

Jencso KG, McGlynn BL, Gooseff MN, Bencala KE, Wondzell SM. 2010. Hillslope hydrologic connectivity controls riparian groundwater turnover: implications of catchment structure for riparian buffering and stream water sources. *Water Resources Research* 46(11): W10524.

- Jencso, K.G. and McGlynn, B.L., 2011. Hierarchical controls on runoff generation: Topographically driven hydrologic connectivity, geology, and vegetation. *Water Resources Research*, 47(11).
- Jenson, S.K. and Domingue, J.O., 1988. Extracting topographic structure from digital elevation data for geographic information system analysis. *Photogrammetric engineering and remote sensing*, 54(11), pp.1593-1600.
- Kampf, S.K., Brogan, D.J., Schmeer, S., MacDonald, L.H. and Nelson, P.A., 2016. How do geomorphic effects of rainfall vary with storm type and spatial scale in a post-fire landscape?. *Geomorphology*, 273, pp.39-51.
- Kienzle, S., 2004. The Effect of DEM Raster Resolution on First Order, Second Order and Compound Terrain Derivatives. *Transactions in GIS* 8(1):83-111.
- Kirkby M. 1975. Hydrograph modelling strategies. In *Processes in Physical and Human Geography*, Peel R, Chisholm M, Haggett P (eds). Heinemann: London; 69–90.
- Kirkby, M., 1988. Hillslope runoff processes and models. *Journal of Hydrology*, 100(1-3), pp.315-339.
- Kirkby, M.J., 1992. Thresholds and instability in stream head hollows: a model of magnitude and frequency for wash processes. School of Geography, University of Leeds.
- Kirkby, M.J., 1993. Long term interactions between networks and hillslopes. *Channel Network Hydrology*, pp.255-293.
- Laio, F., Porporato, A., Fernandez-Illescas, C.P., Rodriguez-Iturbe, I., 2001. Plants in water-controlled ecosystems: active role in hydrologic processes and response to water stress IV. Discussion of real cases. *Advances in Water Resources* 24, 745–762.
- Lea, N.L., 1992. An aspect driven kinematic routing algorithm. *Overland flow: Hydraulics and Erosion Mechanics*, 147, p.175.
- Leopold, M., Völkel, J., Huber, J. and Dethier, D., 2013. Subsurface architecture of the Boulder Creek Critical Zone Observatory from electrical resistivity tomography. *Earth surface processes and landforms*, 38(12), pp.1417-1431.
- Li, J. and Wong, D.W., 2010. Effects of DEM sources on hydrologic applications. *Computers, Environment and urban systems*, 34(3), pp.251-261.
- Lindsay, J.B. and Creed, I.F., 2005a. Removal of artifact depressions from digital elevation models: towards a minimum impact approach. *Hydrological processes*, 19(16), pp.3113-3126.

Lindsay, J.B. and Creed, I.F., 2005b. Sensitivity of digital landscapes to artifact depressions in remotely-sensed DEMs. *Photogrammetric Engineering & Remote Sensing*, 71(9), pp.1029-1036.

Machette, M. N., Birkeland, P. W., Markos, G., Guccione, M. J., 1976, Soil development in Quaternary deposits in the Golden-Boulder portion of the Colorado Piedmont: *Prof. Contrib. Colo. Sch. Mines*, v. 8, p. 217-259.

Mallants, D., Mohanty, B.P., Vervoort, A. and Feyen, J., 1997. Spatial analysis of saturated hydraulic conductivity in a soil with macropores. *Soil Technology*, 10(2), pp.115-131.

Martz, L.W. and Garbrecht, J., 1998. The treatment of flat areas and depressions in automated drainage analysis of raster digital elevation models. *Hydrological processes*, 12(6), pp.843-855.

McIntyre, R.E., Adams, M.A., Ford, D.J. and Grierson, P.F., 2009. Rewetting and litter addition influence mineralisation and microbial communities in soils from a semi-arid intermittent stream. *Soil Biology and Biochemistry*, 41(1), pp.92-101.

McMaster, K.J., 2002. Effects of digital elevation model resolution on derived stream network positions. *Water Resources Research*, 38(4).

McNamara JP, Chandler D, Seyfried M, Achet S. 2005. Soil moisture states, lateral flow, and streamflow generation in a semi-arid, snowmelt-driven catchment. *Hydrological Processes* 19: 4023–4038. DOI:10.1002/hyp.5869.

Meyer, J.L., Strayer, D.L., Wallace, J.B., Eggert, S.L., Helfman, G.S. and Leonard, N.E., 2007. The contribution of headwater streams to biodiversity in river networks. *JAWRA Journal of the American Water Resources Association*, 43(1), pp.86-103.

Montgomery, D.R. and Dietrich, W.E., 1988. Where do channels begin?. *Nature*, 336(6196), p.232.

Montgomery, D.R. and Dietrich, W.E., 1989. Source areas, drainage density, and channel initiation. *Water Resources Research*, 25(8), pp.1907-1918.

Montgomery, D.R. and Dietrich, W.E., 1992. Channel initiation and the problem of landscape scale. *Science*, 255(5046), pp.826-830.

Montgomery, D.R. and Fournelle-Georgiou, E., 1993. Channel network source representation using digital elevation models. *Water Resources Research*, 29(12), pp.3925-3934.

Moore, C. (2012). A climatological study of snow covered areas in the western United States. MS Thesis, Colorado State University, Fort Collins, CO.

Morin, E., Grodek, T., Dahan, O., Benito, G., Kulls, C., Jacoby, Y., Van Langenhove, G., Seely, M. and Enzel, Y., 2009. Flood routing and alluvial aquifer recharge along the ephemeral arid Kuiseb River, Namibia. *Journal of Hydrology*, 368(1), pp.262-275.

Moultrie, W., 1970. Systems, computer simulations, and drainage basins. *Bull. ILL Geogr*, pp.29-35.

Nadeau, T.L. and Rains, M.C., 2007. Hydrological connectivity of headwaters to downstream waters: Introduction of the featured collection. *Journal of the American Water Resources Association*, 43(1), p.1.

NEON, 2013. 'The National Ecological Observatory Network is a project sponsored by the National Science Foundation and managed under cooperative agreement by NEON, Inc. This material is based in part upon work supported by the National Science Foundation under Grant No. DBI-0752017'

Nesse, W.D. and Braddock, W.A., 1989. Geologic map of the Pingree Park quadrangle, Larimer county, Colorado (No. 1622).

Nippgen F, McGlynn BL, Marshall LA, Emanuel RE. 2011. Landscape structure and climate influences on hydrologic response, *Water Resources Research* 47: W12528. DOI:10.1029/2011WR011161.

Niswonger, R.G., Prudic, D.E., Pohll, G. and Constantz, J., 2005. Incorporating seepage losses into the unsteady streamflow equations for simulating intermittent flow along mountain front streams. *Water resources research*, 41(6).

O'Callaghan, J.F. and Mark, D.M., 1984. The extraction of drainage networks from digital elevation data. *Computer vision, graphics, and image processing*, 28(3), pp.323-344.

Omran, A., Dietrich, S., Abouelmagd, A. and Michael, M., 2016. New ArcGIS tools developed for stream network extraction and basin delineations using Python and java script. *Computers & Geosciences*, 94, pp.140-149.

Onda, Y., Komatsu, Y., Tsujimura, M. and Fujihara, J.I., 2001. The role of subsurface runoff through bedrock on storm flow generation. *Hydrological Processes*, 15(10), pp.1693-1706.

Onda, Y., Tsujimura, M., Fujihara, J.I. and Ito, J., 2006. Runoff generation mechanisms in high-relief mountainous watersheds with different underlying geology. *Journal of hydrology*, 331(3-4), pp.659-673.

Orlandini, S., Moretti, G., Franchini, M., Aldighieri, B. and Testa, B., 2003. Path-based methods for the determination of nondispersive drainage directions in grid-based digital elevation models. *Water resources research*, 39(6).

Paybins, K.S., 2003. Flow Origin, Drainage Area, and Hydrologic Characteristics for Headwater Streams in the Mountaintop Coal-Mining Region of Southern West Virginia, 2000-01. Water-Resources Investigations Report 02-4300, U.S. Department of the Interior and U.S. Geological Survey, Charleston, West Virginia.

Payn RA, Gooseff MN, McGlynn BL, Bencala KE, Wondzell SM, 2012. Exploring changes in the spatial distribution of stream baseflow generation during a seasonal recession. *Water Resources Research* 48: W04519. DOI:10.1029/2011WR011552

Pelletier, J. D., 2013. A robust, two-parameter method for the extraction of drainage networks from high-resolution digital elevation models (DEMs): Evaluation using synthetic and real-world DEMs, *Water Resour. Res.*, 49, 75–89, doi:10.1029/2012WR012452.

PRISM Climate Group, 2017. Oregon State University, <http://PRISM.oregonstate.edu>, created 4 Feb 2004.

Qin, C.Z., Zhu, A.X., Pei, T., Li, B.L., Scholten, T., Behrens, T. and Zhou, C.H., 2011. An approach to computing topographic wetness index based on maximum downslope gradient. *Precision Agriculture*, 12(1), pp.32-43.

Quinn, P.F., Beven, K.J. and Lamb, R., 1995. The $\ln(a/\tan\beta)$ index: How to calculate it and how to use it within the topmodel framework. *Hydrological processes*, 9(2), pp.161-182.

Quinn, P.F.B.J., Beven, K., Chevallier, P. and Planchon, O., 1991. The prediction of hillslope flow paths for distributed hydrological modelling using digital terrain models. *Hydrological processes*, 5(1), pp.59-79.

Richer, E.E., 2009. Snowmelt runoff analysis and modeling for the Upper Cache la Poudre River Basin, Colorado. Doctoral dissertation, Colorado State University.

Richer, E.E., Kampf, S.K., Fassnacht, S.R. and Moore, C.C., 2013. Spatiotemporal index for analyzing controls on snow climatology: application in the Colorado Front Range. *Physical Geography*, 34(2), pp.85-107.

Rodriguez-Iturbe I. 2000. Ecohydrology: a hydrologic perspective of climate–soil–vegetation dynamics. *Water Resources Research* 36: 3–9.

Rodriguez-Iturbe I, Valdes JB. 1979. The geomorphic structure of the hydrologic response. *Water Resources Research* 15(6): 1409–1420.

Rueda, A., Noguera, J.M. and Martínez-Cruz, C., 2013. A flooding algorithm for extracting drainage networks from unprocessed digital elevation models. *Computers & geosciences*, 59, pp.116-123.

- Savenije, H.H.G., 2010. HESS Opinions" Topography driven conceptual modelling (FLEX-Topo)". *Hydrology and Earth System Sciences*, 14(12), pp.2681-2692.
- Schäuble, H., Marinoni, O. and Hinderer, M., 2008. A GIS-based method to calculate flow accumulation by considering dams and their specific operation time. *Computers & Geosciences*, 34(6), pp.635-646.
- Schumm, S.A., 1979. *Geomorphic Thresholds: The Concept and Its Applications*. Transactions of the Institute of British Geographers, New Series 4(4):485-515.
- Sklar, L.S. and Dietrich, W.E., 2001. Sediment and rock strength controls on river incision into bedrock. *Geology*, 29(12), pp.1087-1090.
- Sofia, G., P. Tarolli, F. Cazorzi, and G. Dalla Fontana (2011), An objective approach for feature extraction: Distribution analysis and statistical descriptors for scale choice and channel network identification, *Hydrol. Earth Syst. Sci.*, 15(5), 1387–1402, doi:10.5194/hess-15-1387- 2011.
- Soil Survey Staff, 2016. Natural Resources Conservation Service, United States Department of Agriculture. Web Soil Survey. Available online at the following link: <https://websoilsurvey.sc.egov.usda.gov/>. Accessed [11/13/2016].
- Sörensen, R., Zinko, U. and Seibert, J., 2006. On the calculation of the topographic wetness index: evaluation of different methods based on field observations. *Hydrology and Earth System Sciences Discussions*, 10(1), pp.101-112.
- Sörensen, R. and Seibert, J., 2007. Effects of DEM resolution on the calculation of topographical indices: TWI and its components. *Journal of Hydrology*, 347(1), pp.79-89.
- Sprunt, B., 1972. Digital simulation of drainage basin development. *Spatial analysis in geomorphology*, pp.371-89.
- Stanley, E.H., Fisher, S.G. and Grimm, N.B., 1997. Ecosystem expansion and contraction in streams. *BioScience*, 47(7), pp.427-435.
- Stieglitz, M., Shaman, J., McNamara, J., Engel, V., Shanley, J. and Kling, G.W., 2003. An approach to understanding hydrologic connectivity on the hillslope and the implications for nutrient transport. *Global Biogeochemical Cycles*, 17(4).
- Suzanne Anderson, Nathan Rock (2016). "CZO Dataset: Gordon Gulch: Lower - Streamflow / Discharge (2013-2016) - (GGL_SW_0)." Retrieved 17 Jan 2018, from <http://criticalzone.org/boulder/data/dataset/4035/>
- Tague, C. and Grant, G.E., 2004. A geological framework for interpreting the low-flow regimes of Cascade streams, Willamette River Basin, Oregon. *Water Resources Research*, 40(4).

Tarboton, D.G., 1997. A new method for the determination of flow directions and upslope areas in grid digital elevation models. *Water resources research*, 33(2), pp.309-319.

Tarboton, D. G., R. L. Bras, and I. Rodriguez-Iturbe (1991). On the extraction of channel networks from digital elevation data, *Hydrol. Processes*, 5(1), 81–100, doi:10.1002/hyp.3360050107.

Tarboton, D. G., R. L. Bras, and I. Rodriguez-Iturbe (1992). A physical basis for drainage density, *Geomorphology*, 5(1–2), 59–76, doi:10.1016/0169-555X(92)90058-V.

Tarboton, D.G., 2005. *Terrain analysis using digital elevation models (TauDEM)*. Utah State University, Logan.

Uchida, T., Miyata, S. and Asano, Y., 2008. Effects of the lateral and vertical expansion of the water flowpath in bedrock on temporal changes in hillslope discharge. *Geophysical Research Letters*, 35(15).

Uhlenbrook, S., M. Frey, C. Leibundgut, and P. Maloszewski (2002), Hydrograph separation in a mesoscale mountainous basin at event and seasonal timescales, *Water Resour. Res.*, 38(6), 1096, doi:10.1029/2001WR000938.

Usery, E.L. et al, 2004. Geospatial data resampling and resolution effects on watershed modeling: a case study using the agricultural non-point source pollution model. *Journal of Geographical Systems* 6, 289–306.

U.S. Geological Survey, 1991. National Elevation Dataset, U.S. Geological Survey (USGS), EROS Data Center. <<http://gisdata.usgs.net/ned/>>

U.S. Geological Survey, 2013, National Hydrography Geodatabase: The National Map viewer available on the World Wide Web (<https://viewer.nationalmap.gov/viewer/nhd.html?p=nhd>), accessed [10/3/16]

USGS National Geologic Map Database, 2016. U.S. Geological Survey, National Cooperative Geologic Mapping Program. <http://ngmdb.usgs.gov/>

Vaze, J., Teng, J. and Spencer, G., 2010. Impact of DEM accuracy and resolution on topographic indices. *Environmental Modelling & Software*, 25(10), pp.1086-1098.

Villeneuve, S., Cook, P.G., Shanafield, M., Wood, C. and White, N., 2015. Groundwater recharge via infiltration through an ephemeral riverbed, central Australia. *Journal of Arid Environments*, 117, pp.47-58.

- Villines, J.A., Agouridis, C.T., Warner, R.C. and Barton, C.D., 2015. Using GIS to delineate headwater stream origins in the Appalachian coalfields of Kentucky. *JAWRA Journal of the American Water Resources Association*, 51(6), pp.1667-1687.
- Wagener, T., Sivapalan, M., Troch, P. and Woods, R., 2007. Catchment classification and hydrologic similarity. *Geography compass*, 1(4), pp.901-931.
- Western, A. W., R. B. Grayson, G. Bloßchl, G. R. Willgoose, and T. A. McMahon (1999), Observed spatial organization of soil moisture and its relation to terrain indices, *Water Resour. Res.*, 35(3), 797– 810.
- Wharton G., 1994. Progress in the use of drainage network indices for rainfall-runoff modelling and runoff prediction. *Progress in Physical Geography* 18(4): 539–557. DOI: 10.1177/030913339401800404
- Williams, D.D., 2006. *The Biology of Temporary Waters*. Oxford University Press, Oxford, United Kingdom
- Wolock, D.M., Fan, J. and Lawrence, G.B., 1997. Effects of basin size on low-flow stream chemistry and subsurface contact time in the Neversink River watershed, New York. *Hydrological Processes*, 11(9), pp.1273-1286.
- Wolock, D.M., McCabe, G.J., 2000. Differences in topographic characteristics computed from 100- and 1000-m resolution digital elevation model data. *Hydrological Processes* 14 (6), 987–1002.
- Woods, R.A., Sivapalan, M. and Robinson, J.S., 1997. Modeling the spatial variability of subsurface runoff using a topographic index. *Water Resources Research*, 33(5), pp.1061-1073.
- Yimer, F., Ledin, S. and Abdelkadir, A., 2006. Soil property variations in relation to topographic aspect and vegetation community in the south-eastern highlands of Ethiopia. *Forest Ecology and Management*, 232(1), pp.90-99.
- Zhang, W.H., Montgomery, D.R., 1994. Digital elevation model grid size, landscape representation, and hydrologic simulations. *Water Resources Research* 30 (4), 1019–1028.
- Zinko, U., Seibert, J., Dynesius, M. and Nilsson, C., 2005. Plant species numbers predicted by a topography-based groundwater flow index. *Ecosystems*, 8(4), pp.430-441.